frontiers in Marine Science

ORIGINAL RESEARCH
published: 10 February 2022
doi: 10.3389/fmars.2021.799358

Acquired Phototrophy and Its Implications for Bloom Dynamics of the *Teleaulax-Mesodinium-Dinophysis*-Complex

*Anna-A. Anschütz[1,2], Kevin J. Flynn[3] and Aditee Mitra[1]**

[1] School of Earth and Environmental Sciences, Cardiff University, Cardiff, United Kingdom, [2] Écologie des Systèmes Aquatiques, Université Libre de Bruxelles, Brussels, Belgium, [3] Plymouth Marine Laboratory, Prospect Place, Plymouth, United Kingdom

The dinoflagellate *Dinophysis* is responsible for causing diarrhetic shellfish poisoning impacting shellfish aquaculture globally. *Dinophysis* species are invariably plastidic specialist non-constitutive mixoplankton (pSNCM), combining phagotrophy with acquired phototrophy. *Dinophysis* acquires phototrophy from another pSNCM, the ciliate *Mesodinium*, which in turn acquires phototrophy from cryptophytes within the *Teleaulax-Plagioselmis-Geminigera* clade. Despite this trophic linkage, the temporal dynamics of cryptophyte-*Mesodinium-Dinophysis* remain poorly understood. In this study, we present the first *Teleaulax-Mesodinium-Dinophysis* (TMD)-complex system dynamics model. Using this, we explored the dynamics of TMD interactions under different ecological settings. Temperature, nutrient load, mixed layer depth, and irradiance all greatly influenced the timing and magnitude of the TMD-complex interactions and, as a result, *Dinophysis* bloom duration and peak. Availability of *Mesodinium* and temporal matching of its growth to that of *Dinophysis* are also key biotic factors; the timing of *Mesodinium* availability impacts the potential of *Dinophysis* growth for up to 3 months. Integrating our TMD-complex model with a suitable hydrodynamic model could greatly improve our understanding of bloom formation and aid in forecasting harmful algal bloom (HAB) events. Future monitoring of *Dinophysis* would also be enhanced by the monitoring of the precursor prey species, *Teleaulax* and *Mesodinium*, which are rarely accorded the same effort as the HAB forming dinoflagellate.

Keywords: mixoplankton, harmful algal blooms, HABs, systems dynamics modeling, predator-prey, TMD-complex, trophic dynamics

OPEN ACCESS

Edited by:
Manuel F. G. Weinkauf, Charles University, Czechia

Reviewed by:
Daniel Alan Lemley, Nelson Mandela University, South Africa
Mengmeng Tong, Zhejiang University, China

****Correspondence:***
Aditee Mitra
MitraA2@Cardiff.ac.uk

Specialty section:
This article was submitted to Marine Biology, a section of the journal Frontiers in Marine Science

Received: *21 October 2021*
Accepted: *01 December 2021*
Published: *10 February 2022*

Citation:
Anschütz A-A, Flynn KJ and Mitra A (2022) Acquired Phototrophy and Its Implications for Bloom Dynamics of the Teleaulax-Mesodinium-Dinophysis-Complex. Front. Mar. Sci. 8:799358. doi: 10.3389/fmars.2021.799358

INTRODUCTION

Dinophysis is a harmful dinoflagellate of global distribution (**Figure 1**) that is the causative agent for diarrhetic shellfish poisoning (DSP) events leading to the closure of aquaculture facilities (review by Reguera et al., 2012, 2014). Significant effort has been expended on understanding the dynamics behind the occurrence of these, and other harmful algal bloom (HAB), events to find ways to forecast them (Raine et al., 2010; Velo-Suárez et al., 2010; Ajani et al., 2016; Moita et al., 2016;

Pinto et al., 2016); many monitoring programs target toxigenic *Dinophysis* species (Campbell et al., 2010). Traditional methods of monitoring *Dinophysis* by counting cells and using satellite chlorophyll concentrations are not robust for forecasting blooms of these species (Ruiz-Villarreal et al., 2016). This is because the cell concentration threshold for *Dinophysis*, at which this organism can pose a threat, is only 200 cells L^{-1} (Yasumoto et al., 1985), a cell abundance level that can be very difficult to detect (Berdalet et al., 2017). Satellite imagery is inappropriate because blooms often occur in subsurface water layers and are, therefore, not detectable with this method (e.g., *Dinophysis acuta*; Ruiz-Villarreal et al., 2016).

Modeling offers tools to forecast blooms and also to aid understanding of the dynamics behind their occurrences (Cusack et al., 2016; Ruiz-Villarreal et al., 2016; Flynn and McGillicuddy, 2018). Most models for *Dinophysis* bloom formation emphasize the importance of physical oceanographic drivers (Raine et al., 2010; Velo-Suárez et al., 2010; Moita et al., 2016; Pinto et al., 2016), with a particular focus on upwelling and downwelling processes and coastal advection that bring *Dinophysis* cells into coastal waters from offshore, or into surface waters from deeper water layers (**Table 1**). However, there is still a lack of predictive power in the existing models suggesting that there may be one or more key features missing from these models, for example, the biological characteristics (Ajani et al., 2016; Moita et al., 2016).

An important aspect of *Dinophysis* is that most of the toxigenic species (Anderson et al., 2002; Park et al., 2006; Jaén and Mamán, 2009; Nishitani et al., 2010; Rodríguez et al., 2012) are mixoplanktonic (Leles et al., 2017). Mixoplankton are protists that employ photosynthesis and phagotrophy for their nutritional needs (Flynn et al., 2013, 2019). There are important differences between mixoplankton functional types which greatly complicate the mechanistic modeling of these organisms (Mitra and Flynn, 2010; Mitra et al., 2016). *Dinophysis* sp. is plastidic specialist non-constitutive mixoplankton (pSNCM, defined by Mitra et al., 2016, modified by Flynn et al., 2019) that acquire their phototrophic ability from ingestion of ciliates from the *Mesodinium* genus (e.g., *Mesodinium rubrum*, Park et al., 2006; *Mesodinium major*, Rial et al., 2015; *Mesodinium chamaeleon*, Moeller et al., 2021; *Mesodinium coatsi*, Nam et al., 2015). *Mesodinium* is itself a pSNCM and acquires phototrophic potential from consumption of cryptophytes from the *Teleaulax-Plagioselmis-Geminigera* (TPG) clade (Gustafson et al., 2000; Johnson et al., 2006; Hernández-Urcera et al., 2018). However, there are records of *Mesodinium* and, as a result, *Dinophysis* (using *Mesodinium* as an intermediate), acquiring phototrophy using cryptophytes outside of the TPG clade (Díaz et al., 2020; Moeller et al., 2021). The cryptophyte *Teleaulax* are constitutive mixoplankton (CM; Mitra et al., 2016; Flynn et al., 2019), having their own innate photosystems, and can feed on bacterioplankton and the cyanobacterium *Synechococcus* (Yoo et al., 2017). While both the pSNCM (ciliate and dinoflagellate) are capable of maintaining their acquired phototrophy (kleptoplastids) for some time, ultimately they rely on this trophic linkage to proliferate (Hansen et al., 2013). Despite this strict linkage within the TMD-complex, while the global distribution and occurrence of *Dinophysis* are well-recorded, the distribution of *Mesodinium* is less well-documented, and this is even less so for *Teleaulax* (**Figure 1**). However, due to the species-specific plastid requirements of *Dinophysis*, the distribution of *Mesodinium* and also *Teleaulax* may be expected to be as widespread as *Dinophysis*.

Blooms of *Mesodinium* and *Dinophysis* can occur a couple of weeks apart, assuming that sufficient prey in the form of a *Mesodinium* bloom is available to support the initial *Dinophysis* growth (Moita et al., 2016). This is possible because *Mesodinium* retains the prey nuclei for acquired phototrophy with a half-life of 10 days or so and can maintain plastids potentially for months (Park et al., 2008). Accordingly, it has been suggested (Harred and Campbell, 2014) to use the presence of *M. rubrum* as an indicator for blooms of *Dinophysis ovum* in the Gulf of Mexico. There have been suggestions of including *Mesodinium* and their cryptophyte prey in the modeling of *Dinophysis* blooms (e.g., Glibert et al., 2010). While the conceptual model for the Rias in NW Spain combines physical oceanographic drivers with *Mesodinium-Dinophysis* occurrence to improve predictions of *Dinophysis* blooms (Velo-Suárez et al., 2014), first and foremost such blooms depend on the unique relationship the *Dinophysis* have with their prey. To further explore the dynamics of this biological complex formed of *Teleaulax-Mesodinium-Dinophysis* (hereafter TMD-complex) requires a simulation model that focuses on the unique physiology of the three organisms. Hitherto, however, there has been no attempt to mechanistically model these interactions.

In this study, we present the first system dynamics model describing the functioning of the TMD-complex. For the *in silico* experiments, the *Dinophysis* component was configured as *Dinophysis acuminata* because it is a well-studied common toxigenic species. There are relatively more physiological data available for this particular species to aid model configuration. *Teleaulax amphioxeia* and *Mesodinium rubrum* were chosen as species representatives for the cryptophyte and *Mesodinium* components, respectively, as these are associated with acquired phototrophy of *D. acuminata*. However, it must be noted that the TMD-complex model is designed on the ecophysiological understanding of these organisms; being a system biology-based platform, the model can be configured for different TMD species. We conducted *in silico* experiments using this configuration to explore the dynamics of the TMD-complex in response to predator-prey ratios, under different environmental conditions, such as nutrient concentrations, irradiance, and temperature. This food-web simulator focuses on the effect of the unique biology and interactions between the different mixoplankton types of the complex. From a conceptual angle, the model thus also proves a platform for improving our understanding of any future new-found mixoplankton interactions involving the exchange of phototrophic potential. Furthermore, the relatively simple construct of the TMD-complex model offers the potential for future coupling of this to a hydrodynamic model.

MATERIALS AND METHODS

What follows is a general description of the simulation model. The complete equation set of the model and additional information are provided in the **Supplementary Material**.

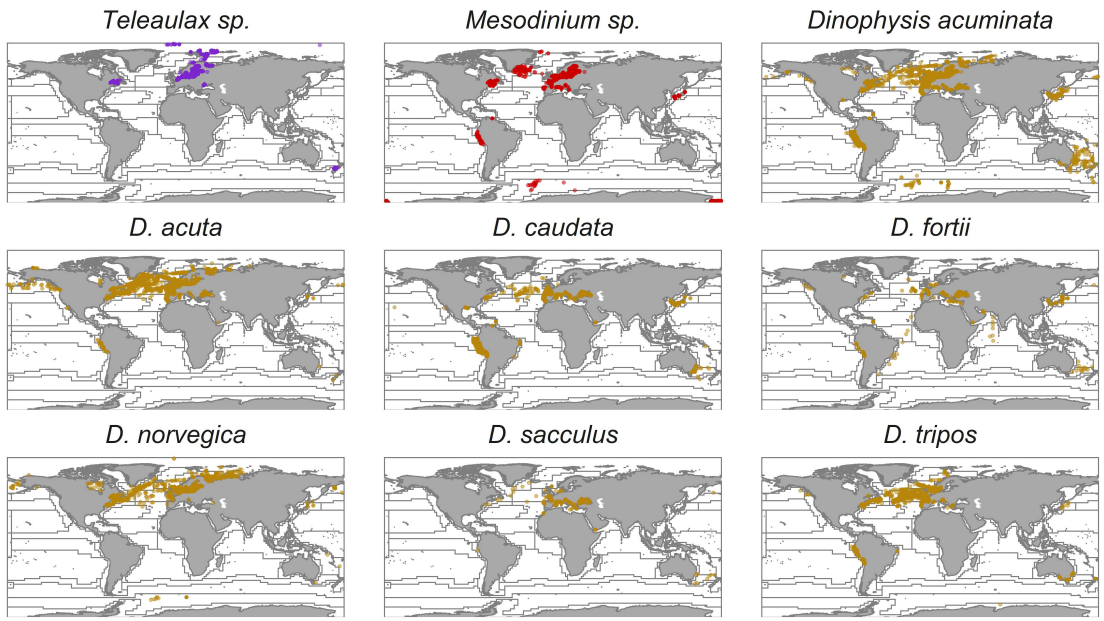

FIGURE 1 | Global distribution of *Teleaulax*, *Mesodinium,* and *Dinophysis* species. Records of *Dinophysis ovum* are merged with *Dinophysis acuminata* as they are likely the same species (Park et al., 2019). The data were obtained from the Ocean Biogeographic Information System (OBIS) database, and the Longhurst provinces were added as described in Leles et al. (2017). Each dot represents a recorded observation.

TABLE 1 | Examples of modeling studies reporting facets of growth dynamics and ecology of *Dinophysis* and *Mesodinium*.

Region	Role	Model description	Target species	References
Irish, Swedish, Dutch coastal waters	Fuzzy logic	Fuzzy logic modeling of HABs	*Dinophysis* spp.	Blauw et al., 2006
Western Andalucía (Spain)	Forecasting	Artificial neural network approach	*D. acuminata*	Velo-Suárez and Gutiérrez-Estrada, 2007
Bantry Bay (Ireland)	Hindcasting and forecasting	3D Physical model (wind); no explicit mixoplankton	*D. acuminata*	Raine et al., 2010
Bay of Biscay (France)	Forecasting	3D Lagrangian Particle-Tracking Model + IBM; no explicit mixoplankton	*D. acuminata*	Velo-Suárez et al., 2010
Thermaikos Gulf (NW Aegean Sea)	Forecasting	2D hydrodynamic model coupled with transport model simulating HAB dispersion including some biological processes with temperature, light and nutrients	*Dinophysis* spp.	Savvidis et al., 2011
Galician Rías Baixas (NW Spain)	Conceptual	2D Physics (wind, up, and downwelling); mismatch of *D. acuminata* and *M. rubrum*	*D. acuminata*	Velo-Suárez et al., 2014
Arabian Sea (India)	Statistical	Generalized linear model	*Dinophysis* sp.	Singh et al., 2014
Bantry Bay (Ireland)	Forecasting	3D physical model: BANTRY model (200–250 m horizontal resolution with 20 vertical levels; no explicit mixoplankton	*Dinophysis* spp.	Cusack et al., 2016
Iberian coast (Europe)	Forecasting	3D Lagrangian particle-tracking model	*D. acuminata*	Pinto et al., 2016
NW Iberia (Europe)	Forecasting	3D Lagrangian offline model + IBM; no explicit mixoplankton	*D. acuminata*, *D. acuta*	Moita et al., 2016
SE Australia	Physico-chemical	Generalized additive models	*D. acuminata*, *D. caudata*, *Mesodinium rubrum*	Ajani et al., 2016
Generic	Conceptual exploration	Biological simulation comparing phototroph and heterotroph with acquired phototroph	*M. rubrum*	Moeller et al., 2016
Generic	System dynamics	Biological simulation of the TMD-complex	*Teleaulax* spp., *Mesodinium* spp., *Dinophysis* spp.	This paper

Model Structure

The TMD food-web simulator is a development of the N-based system dynamics model of mixoplankton functional types described by Anschütz and Flynn (2020). For this study, the original model was extended to describe three protist functional types, namely, two pSNCM (configured for *Mesodinium* and

Dinophysis) and one CM for *Teleaulax*. From here on, these organisms are referred to by their genus name only except when discussing specific species. Generic phytoplankton (termed "Alga"; equivalent spherical diameter, ESD = 6 μm) was included as an additional prey for *Mesodinium* and to provide competition to the *Teleaulax* for nutrients and light in phototrophic growth.

The full construct is shown in **Figure 2**. The food-web comprised the CM *Teleaulax* feeding only on the cyanobacteria *Synechococcus* (Yoo et al., 2017), the pSNCM *Mesodinium* feeding on the CM *Teleaulax*, *Synechococcus,* and the generic phytoplankton Alga (Myung et al., 2006; Jeong et al., 2015), while *Dinophysis* fed only on *Mesodinium*. *Synechococcus* is configured as a generic species representative of a picophytoplankton competitor and potential prey for *Teleaulax*. Dissolved inorganic nutrients (DIN) were described *via* two-state variables representing nitrate (NO_3^-) and ammonium (NH_4^+). All the plankton functional types could uptake NH_4^+. All except *Dinophysis* could also use NO_3^- as this genus seems unable to use this N-source (Hattenrath-Lehmann et al., 2015; García-Portela et al., 2020). However, the construct of the *Dinophysis* model is based on the generic construct of a pSNCM (Anschütz and Flynn, 2020) and, therefore, should evidence of *Dinopysis* using NO_3^- become available, then the model can be readily modified to enable NO_3^- uptake for *Dinophysis* just as it is enabled for the other pSNCM, *Mesodinium*. Nutrient regeneration occurs in the simulator by an implicit regeneration term. Bacteria and the microbial loop components are not explicitly described.

The operational maximum growth rate for each organism (UmT) was calculated with reference to the current temperature (T), the reference temperature (RT) at which the reference growth rate was declared (UmRT), and a Q_{10} factor.

$$UmT = \mathrm{UmRT} \cdot Q_{10}\frac{\mathrm{T}-\mathrm{RT}}{10} \quad (1)$$

A constant loss rate through mortality (0.05 day^{-1}) was applied to all organisms. In the case of *Mesodinium* and *Dinophysis*, this constant mortality was in addition to the mortality rate, described in the original model, accounting for a failure in photosystem activity (Anschütz and Flynn, 2020).

In addition to the two-state variables describing DIN (i.e., nitrate and ammonium), two additional state variables were added describing labile and semi-labile dissolved organic nitrogen (lDON and slDON; **Figure 2**). These accounted for outflows of voided material from predation, releasing organic nitrogen due to mortality and DON leakage concurrent with photosynthesis (Alldredge et al., 1993; Bronk, 1999; Passow, 2002). Both lDON and slDON were decomposed to ammonium at a rate of 0.5 day^{-1}. The exact value of this regeneration did not affect the outcomes of simulations. Cyanobacteria, including *Synechococcus* (Wawrik et al., 2009), and most if not all protist plankton (Flynn and Butler, 1986; Flynn et al., 2019) are capable of exploiting lDON to support their growth. Thus, we enabled

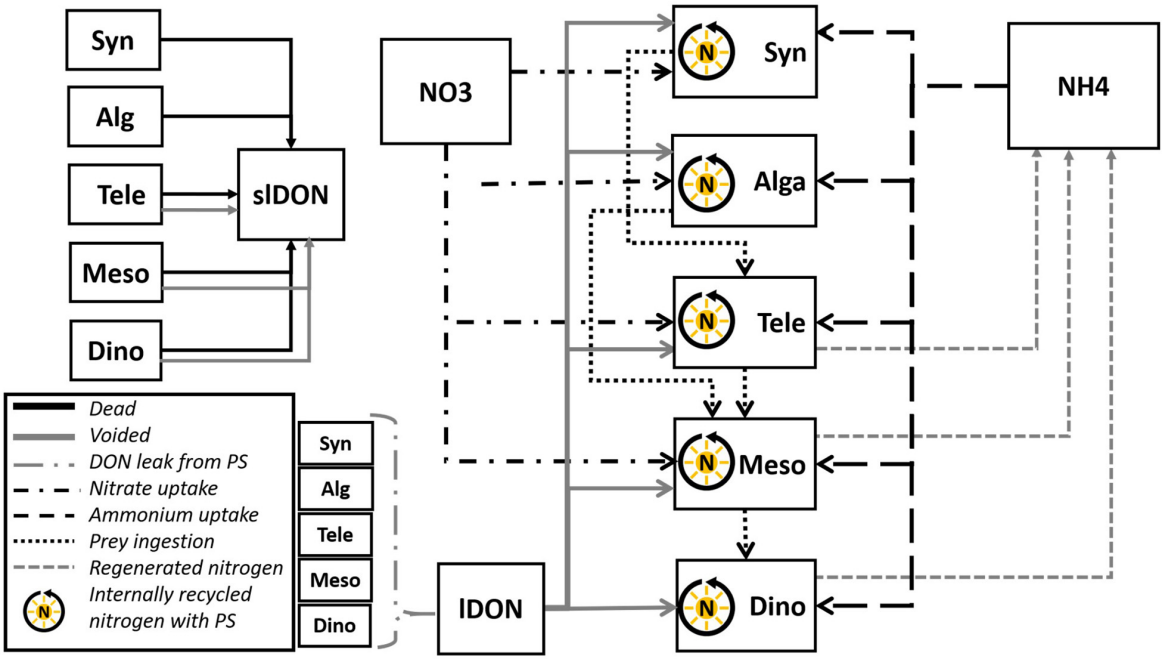

FIGURE 2 | Schematic of the *Teleaulax-Mesodinium-Dinophysis* (TMD)-complex food-web simulator. The model comprises four state variables describing the nutrient sources nitrate (NO3), ammonium (NH4), and lDON and slDON. It also includes five state variable descriptions of plankton functional types (PFT)—a constitutive mixoplankton *Teleaulax* (Tele), two plastidic specialist non-constitutive mixoplankton *Mesodinium* (Meso) and *Dinophysis* (Dino), the cyanobacteria *Synechococcus* (Syn), and generic protist phytoplankton (Alga). All the five PFTs are mixotrophic by virtue of engaging in photosynthesis and heterotrophic use of DON; however, only Tele, Meso, and Dino can engage in phagotrophy and are thus mixoplanktonic. All organisms leak DON. Nitrate (NO3) is available for use by all PFTs except *Dinophysis*. Voided and dead organic material contributes to the DON pools; these degrade to ammonium (NH4) *via* an implicit microbial loop.

all organisms to use lDON with a modification of the routine used by Fasham et al. (1990). Details of model modifications and additions are provided in the **Supplementary Material**.

Model Parameterization

In this study, the model presented was configured specifically to represent *D. acuminata*, assuming a nitrogen content of 2,318 pg N cell^{-1} (cellular carbon content after Menden-Deuer and Lessard, 2000; cellular N:C ratio of *D. acuminata* after Rao and Pan, 1993). *D. acuminata* was chosen for model configuration because it is a common toxigenic species (**Figure 1**), and relatively more physiological data are available to aid model configuration. *T. amphioxeia* and *M. rubrum* were chosen as representatives for the cryptophyte *Teleaulax* and the ciliate *Mesodinium*, respectively, for the same reasons of data availability for the configuration of the model and also as the species associated with acquired phototrophy in *D. acuminata*. If the model was to be used to describe other species, then values for constants controlling physiological features would need to align with traits of those species (**Supplementary Data Sheet 1 Table S1**).

All constant parameters defining the activity of *Synechococcus* sp., *T. amphioxeia*, *M. rubrum,* and *D. acuminata* were accorded values consistent with literature data (**Table 2**). Cellular nitrogen to carbon ratios (N:C) vary among species, with the availability of external nutrients and (for predators) with prey quantity and quality. In this N-based model, the assumed N:C value was constant with the value based on literature data of organisms grown in balanced nutrient conditions. In Anschütz and Flynn (2020), the prey-predator encounter model assumed swimming speeds calculated with reference to cell radius (Flynn and Mitra, 2016). As the motilities (swimming speed; v) of organisms in the TMD-complex organisms are well-studied (Jiang and Johnson, 2021; **Supplementary Data Sheet 1 Table S1**), and in the case of *M. rubrum* is also unique with a high escape swimming speed (Riisgård and Larsen, 2009), the auxiliary controlling motility (in Anschütz and Flynn, 2020) was changed to a constant (v, m s^{-1}) reflecting literature values (**Table 2**). The two pSNCM organisms, *M. rubrum* and *D. acuminata*, have different abilities to maintain optimal functionality of their photosystems which they acquire from their prey; accordingly, these were configured using literature values (*critIR_Meso* and *critIR_Dino* for *M. rubrum* and *D. acuminata* respectively, **Table 3**).

Dynamic Sensitivity Analysis

The dynamic sensitivity analysis was performed in the same manner as described by Anschütz and Flynn (2020). The conditions under which the food-web simulator was run are listed in **Supplementary Data Sheet 1 Table S2**, and the parameters tested for the sensitivity analysis are listed in **Supplementary Data Sheet 1 Table S3**.

In silico Experiment Scenarios

The TMD-complex food-web simulator was developed and run within Powersim Studio 10[1] using an Euler integration routine of step size 0.0625 day^{-1}. Simulations were run with default conditions (unless otherwise noted) of 15°C and surface PFD 500 μmol m^{-2} s^{-1}. Other abiotic conditions were set as described in **Tables 3**, **4**. Steady-state and dynamic sensitivity analyses were conducted as in the study by Anschütz and Flynn (2020).

For most simulations, the mixed layer depth (MLD) was set to 10 m. *Dinophysis* often forms high-density blooms in thin subsurface layers as a result of stratification (Gentien et al., 1995; Anderson et al., 2005; Farrell et al., 2012; Moita et al., 2016). To simulate the physical conditions of a thin layer for subsurface blooms of *D. acuminata* (e.g., Baldrich et al., 2021), the MLD was set to 1 m and irradiance (*de facto* at the top of that thin layer) to 50 μmol m^{-2} s^{-1} to account for the light attenuation in the overlying water.

In most of the scenarios, *Dinophysis* was not subjected to grazing by a higher predator (i.e., there was no closure function applied to this submodel; cf. Mitra, 2009). This was because this study explores the specific interactions within the TMD-complex rather than the complete ecosystem. To test the impact of a grazer of *Dinophysis* on the overall bloom dynamics of the TMD-complex, a simple *Dinophysis* specific grazing function (closure term) implicitly describing activity by a higher predator was implemented. *In silico* experiments at different nutrient loadings were conducted with and without this grazing function. All other simulations were run without this grazing function.

The control (default) scenario was run at eutrophic conditions (700 mgN m^{-3}), 15°C, 10 m MLD, and PFD 500 μmol photons m^{-2} s^{-1}. In all other treatments, one of these factors was changed (**Table 4**). Relative changes in peak biomass and changes in bloom duration were calculated with reference to the control. The organisms, namely, *Synechococcus* sp., generic phytoplankton "Alga," *Teleaulax*, *Mesodinium*, and *Dinophysis,* were inoculated at biomass abundances equivalent to 2, 2, 1.5, 0.1, and 0.01% of initial DIN concentrations, respectively. The biomasses of all organisms were described in nitrogen biomass units (mg N m^{-3}). The complete list of configurations for each *in silico* experiment is given in **Table 4**.

To aid contextual understanding, *Dinophysis* blooms are expressed as cells L^{-1} in addition to biomass. For this transformation, cellular (i.e., biomass) carbon was computed from cellular nitrogen assuming cellular C:N as per the Redfield ratio. Then, cellular carbon was converted to ESD using the equations of Menden-Deuer and Lessard (2000). These values were then used to compute cells L^{-1}.

RESULTS

Biotic Interactions

To provide a reference point for comparisons between different test scenarios, a summary of results is shown in **Figure 3**. All simulations shared a common pattern of organism succession where *Synechococcus* was grazed down early to low residual biomass, followed by growths of "Alga" and *Teleaulax* which were then followed by *Mesodinium* (**Figures 4–8**). The accumulating *Mesodinium* biomass not only outcompeted these species for nutrients but also exerted grazing pressure on them. The

[1]www.Powersim.com

TABLE 2 | Values of constants used to configure the *Synechococcus* (Syn), *Teleaulax* (Tele), *Mesodinium* (Meso), and *Dinophysis* (Dino) submodels.

Parameter	Description	Unit	Species	Value	References
Alpha	Slope of Chl-specific photosynthetic efficiency curve	(m^2 g^{-1} chl.a) × (gC μmol^{-1} photon)	Syn	5.56E-06	Prézelin and Schofield, 1989
			Tele	2.31E-06	Anschütz et al., unpublished
			Meso	5.05E-06	Johnson and Stoecker, 2005
			Dino	4.22E-06	Hansen et al., 2013
BR	Basal respiration	dl	Syn	ca 5% of the umax	Grobbelaar et al., 1991
ChlC	Chlorophyll to carbon ratio	gChl (gC)$^{-1}$	Syn	0.042	Broddrick et al., 2019
			Meso	0.055	Hansen et al., 2013; Rial et al., 2013
			Dino	0.045	Olenina et al., 2006; Hansen et al., 2013
Crit_IR	Max time between ingestions of 1 prey cell per SNCM cell to enable max PS	d^{-1}	Meso	25	Johnson and Stoecker, 2005
			Dino	5	Hansen et al., 2013
Kno3	Half saturation constant for nitrate	mgN m^{-3}	Syn	20.02	Franck et al., 2003
NC	Nitrogen to carbon ratio	gN gC^{-1}	Syn	0.133	Turpin and Miller, 1985
			Tele	0.167	Meunier et al., 2013
			Meso	0.265	Moeller et al., 2011
			Dino	0.125	Rao and Pan, 1993
r	Equivalent spherical radius	μm	Syn	0.98	Yoo et al., 2017
			Tele	6/2	Olenina et al., 2006; Yoo et al., 2017; Anschütz et al., unpublished
			Meso	36/2	Olenina et al., 2006; Montagnes et al., 2008
			Dino	127/2	Larsen and Moestrup, 1992; Bérard-Therriault et al., 1999; Suzuki et al., 2009; Rodríguez et al., 2012
relMaxPrey	Maximum prey:predator size ratio	dl	Tele	1/3	Anschütz et al., unpublished; Yoo et al., 2017
			Meso	5.6/13	Yoo et al., 2017
			Dino	60/78	Olenina et al., 2006; Montagnes et al., 2008
relMinPrey	Minimum prey:predator size ratio	dl	Tele	0.9/7.5	Anschütz et al., unpublished; Yoo et al., 2017
			Meso	3.9/36	Olenina et al., 2006
			Dino	15/176	Olenina et al., 2006; Montagnes et al., 2008
relOpPrey	Optimal prey:predator size ratio	dl	Tele	0.95/6	Anschütz et al., unpublished; Yoo et al., 2017
			Meso	2.2/60	Olenina et al., 2006; Yoo et al., 2017
			Dino	36/127	Olenina et al., 2006; Montagnes et al., 2008
Umax	Maximum growth rate	N N^{-1} d^{-1}	Syn	0.7	Campbell and Carpenter, 1986
			Tele	0.85	Anschütz et al., unpublished; Hamilton et al., 2017
			Meso	0.52	Yih et al., 2004
			Dino	0.535	Kim et al., 2008; Smith et al., 2018
V	Speed of motility	m s^{-1}	Tele	5.55E-05	Meunier et al., 2013
			Meso	5.00E-03	Riisgård and Larsen, 2009
			Dino	1.04E-04	Jiang et al., 2018

If not listed, the values for the respective organism were not found in the literature, and the value from the Anschütz and Flynn (2020) model was used. These values were kept constant in all simulations and during the dynamic sensitivity analysis. Anschütz et al. (unpublished) refer to data obtained from experiments conducted on Teleaulax amphioxeia grown in nitrogen-limited conditions.

ciliate always generated the highest biomass. *Dinophysis* growth started during the active growth phase of *Mesodinium* and then exerted grazing pressure on *Mesodinium* accelerating its eventual decline. Ultimately, both *Mesodinium* and *Dinophysis* declined as their growth rates decreased due to the subsequential loss of their source of acquired phototrophy over time. The top-down control on *Mesodinium* by *Dinophysis* would alleviate the grazing pressure of the ciliates on the cryptophytes; this enables the cryptophytes to bloom again.

Ammonium was used preferentially over nitrate, along with lDON (**Figures 4–8**). Both lDON and slDON accumulated and ammonium began to increase due to the decomposition of these organic forms. High levels of ammonium later in the simulations could not be used by *Mesodinium* and *Dinophysis* because the ultimate source of their chloroplasts, *Teleaulax*, was depleted and, thus, the two pSNCM species lost their ability to photosynthesize, and therefore, could no longer exploit inorganic nutrients (DIN). Depending on the timing of events within the 90-day simulation period, in some simulations, this collapse of the pSNCM allowed *Synechococcus*, Alga, and *Teleaulax* to bloom again.

By the time *Dinophysis* blooms, nitrate concentrations were already much lower or depleted due to prior use by the other

TABLE 3 | Abiotic parameters of the model. Numbers in bold are the values used by default in the simulations (**Figures 3–8**); others are those tested in the dynamic risk analysis (**Supplementary Data Sheet 1 Figure S1**; see also **Table 4**).

Parameter name	Description	Unit	Value
critIR_Meso (DSA)	Critical plastid retention time	d	15; **25**
critIR_Dino (DSA)	Critical plastid retention time	d	**5**; 15; 30
Opt_CR_Meso	Proportion of prey of optimal characteristics captured by starved *Mesodinium*	Dimensionless	**0.2**; 0.5
Opt_CR_Dino	Proportion of prey of optimal characteristics captured by starved *Dinophysis*	Dimensionless	**0.2**; 0.5
LD	Fraction of day as light	Dimensionless	0.7

organisms (**Figures 3**, **4**). However, as the (initial) nutrient load greatly affected the bloom development of those earlier organisms, it affected the timing and magnitude of the much later occurring *Dinophysis* bloom (**Figure 4**). Also, the earlier plankton activity caused ammonium to accumulate, which *Dinophysis* can use while it cannot use nitrate. Oligotrophic conditions (i.e., DIN < 5 μM) did not enable any significant growth of *Dinophysis* nor of any blooms (**Figures 3**, **4**). *Teleaulax* and *Mesodinium* consumed the population of *Synechococcus*. *Teleaulax* and Alga bloom together and were followed by *Mesodinium*. Mesotrophic conditions in the same depth gave rise to a bloom of *Mesodinium* as well as *Dinophysis* (**Figures 3**, **4**). Inorganic nutrient concentrations declined most rapidly when *Mesodinium* reached large biomasses. Eutrophic conditions resulted in the highest cell numbers of *Dinophysis* (**Figure 4**). More nutrients drove earlier, sharper, and higher peak blooms.

In this study, most of the simulations presented featured no grazing pressure on *Dinophysis*, in order to focus on the trophodynamics of the TMD complex. In reality, *Dinophysis* experiences grazing pressure from copepods and other protozooplankton, such as *Fragilidium duplocampanaeforme* (Kozlowsky-Suzuki et al., 2006; Lee and Park, 2017). **Figure 4** shows the consequence of including a generic grazing function for *Dinophysis*. The bloom dynamics of the complex including biomass yield of *Teleaulax* and *Mesodinium* and the timing of the blooms were affected very little by predators grazing on *Dinophysis*. The *Mesodinium* bloom lasted slightly longer in eutrophic conditions. The *Dinophysis* blooms began at the same time but had a much lower biomass yield that is closer to the cell numbers observed in the field.

The proportions and concentrations of each organism at the start of simulations affected both the maximum cell numbers of all organisms and bloom dynamics in terms of bloom peak and duration to varying degrees (**Figures 3**, **5**). Initial higher proportions of *Synechococcus* greatly increased the biomass of *Teleaulax* and to a small extent also that of *Mesodinium* while it had a negligible effect on *Dinophysis* growth (**Figures 3**, **5**). Small initial concentrations of *Mesodinium* in proportion to *Dinophysis* resulted in the largest biomass of *Mesodinium* and the smallest biomass of *Dinophysis* (**Figure 3**), as *Dinophysis* could not develop and, in fact, initially declined (died) due to low prey availability. In consequence, *Dinophysis* could not exert significant grazing pressure on *Mesodinium* later on in the simulation. In contrast, a high initial concentration of the ciliate promoted a more rapid sequence of events that eventually (because both *Mesodinium* and *Dinophysis* blooms crashed) led to a later bloom of *Synechococcus* that used the available regenerated ammonium. High concentrations of *Dinophysis* inoculum promoted a quick bloom succession with smaller maximum biomasses of all organisms and no succeeding blooms (**Figures 3**, **5**).

Abiotic Interactions

Higher irradiance increased the peak size of blooms of each organism type and also prolonged the bloom duration (**Figure 3**), but the timing of their blooms did not change (**Figure 6**). In contrast, temperature increases had a large effect on the

TABLE 4 | Abiotic parameters of the model were varied in the simulations.

Parameter name	Description	Unit	Value					Figure
N_load	Nutrient load	mg N m^{-3}	70 (oligotrophic); 280 (mesotrophic); **700 (eutrophic)**					4
Synechococcus (S) Alga (A) *Teleaulax (T)* *Mesodinium (M)* *Dinophysis (D)*	Organism inoculations tested, shown in the format *S-A-T-M-D*, with initials indicating the species	% of initial DIN (mg N m^{-3})		**S**	**A**	**T**	**M**	**D**	5
			Original	**2**	**2**	**1.5**	**0.1**	**0.01**	
			+S	10	2	1.5	0.1	0.01	
			-T	2	2	0.5	0.1	0.01	
			-M	2	2	1.5	0.01	0.01	
			+M	2	2	1.5	1	0.01	
			+D	2	2	1.5	0.1	0.1	
PFD	Surface light irradiance	μmol m^{-2} s^{-1}	50; 100; **500**; 1000						6
T	Temperature	°C	5; 10; **15**; 20						7
MLD	Mixed layer depth	m	1; **10**						8

Values in bold are those used by default (i.e., control). In each figure, only one parameter was changed, using the value(s) in plain face. The nutrient load levels (70, 280, and 700 mgN m^{-3}) were the same as in Anschütz and Flynn (2020) and equate to 5, 20, and 50 μM N, respectively.

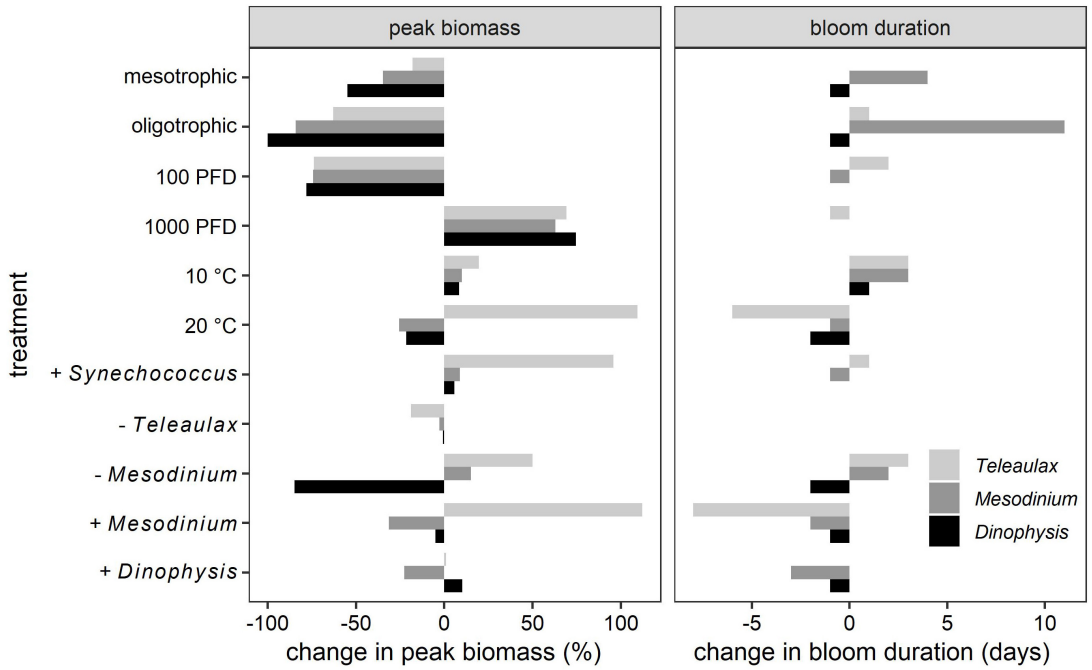

FIGURE 3 | Impact of different abiotic and biotic factors on the simulated TMD-complex bloom dynamics. Left panel, differences in peak biomass relative to the default (control). Right panel, absolute differences in bloom duration from control. "+" and "−" indicate an increase or decrease in the species inoculum, respectively (see also **Table 4**).

outcome of the *Dinophysis* bloom with the potential to accelerate the appearance of its bloom as well as decrease its duration (**Figures 3**, **7**). In addition, these factors promoted earlier blooms of *Dinophysis* and shorter growth cycles, but they could also lower the maximum cell numbers. The lower the temperature, the more the peak of *Dinophysis* was delayed (several days or weeks). The cell numbers of the *Dinophysis* bloom varied with the phase of the *Mesodinium* bloom in which *Dinophysis* began to grow.

In the comparison of the simulations at 10 m MLD vs. 1 m MLD, the maximum biomass of all organisms was lower at 10 m MLD, except *Synechococcus* which was grazed away early in all instances (**Figure 8**). The duration of the individual blooms remained broadly similar, but in 10 m MLD nitrate concentrations did not decline to the same low level as in the 1 m depth simulation. The predator-prey encounter rates were higher in 1 m depth. While the encounter rates between *Teleaulax* and *Synechococcus* are roughly the same in 1 m and 10 m depths, the encounter rate between *Mesodinium* and *Teleaulax* was almost double within the 1 m thin layer simulation. The encounter between *Dinophysis* and *Mesodinium* was also higher in 1 m depth and began to increase earlier than in 10 m.

Overall, *Teleaulax* peak biomass increased under any conditions that decreased the biomass of *Mesodinium* (**Figure 3**). While higher temperature increased the peak biomass of *Teleaulax*, it decreased that of *Mesodinium* and *Dinophysis*. Higher irradiance raised the peak biomass of all three organisms. Changes in the peak biomass of *Teleaulax* and *Mesodinium* were often coupled with the opposite effect in bloom duration. For example, while lower nutrient concentrations decreased and higher irradiances increased peak biomasses, bloom duration increased and decreased, respectively (**Figure 3**). In *Dinophysis*, there was much less variation in bloom duration compared with *Teleaulax* and *Mesodinium*.

DISCUSSION

Understanding the bloom dynamics of the TMD complex is greatly complicated by the multitude of biotic and abiotic factors. These include water column stratification, salinity, advection of organisms and nutrients, changes in predator-prey interactions, and the mixoplanktonic nature of the organisms. In this study, we focused specifically on the interaction between the organisms of the TMD-complex itself. Thus, we assumed a simplified mesocosm-like situation to constrain impacts of hydrodynamics and higher predatory activity. We took this approach because, ultimately, blooms of *Dinophysis* can only develop if the other members of the TMD-complex have already proliferated and are present in the environment. Thus, *Dinophysis* depends mostly on the availability of *Mesodinium* at the right time. Likewise, *Mesodinium* depends on the cryptophyte or similar prey for its acquired phototrophy.

In our simulations, abiotic factors, directly and indirectly, shaped the timing and magnitude of *Dinophysis* blooms as they influenced the development of the *Mesodinium* bloom from which *Dinophysis* itself started to proliferate. The effects of the initial conditions accumulate over time and lead to, sometimes, counter-intuitive results. The collective interactions

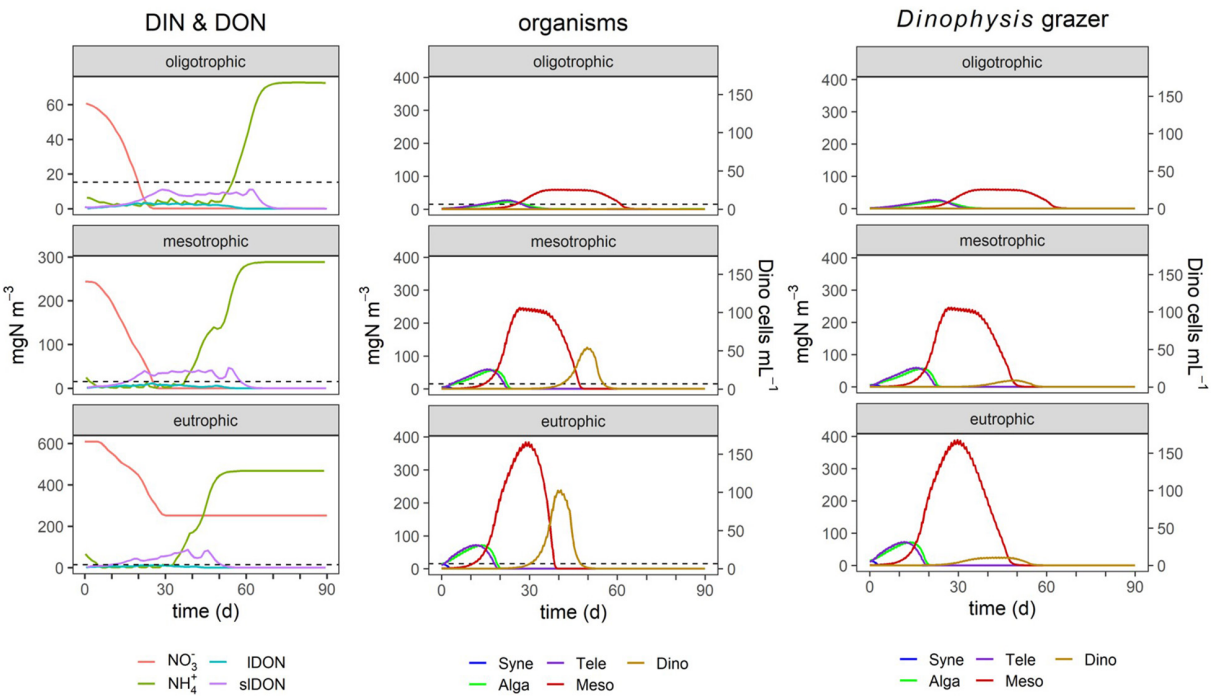

FIGURE 4 | Effect of nutrient loading on TMD dynamics. The nitrogen concentration loads were 70 mgN m^{-3} (oligotrophic), 280 mgN m^{-3} (mesotrophic), and 700 mgN m^{-3} (eutrophic). Cell numbers for *Dinophysis* (secondary *y*-axis) were transformed from nitrogen biomass assuming the cell size of *D. acuminata*; see the "Materials and Methods" section. Legend identifications are as follows: Syne, *Synechococcus* sp.; Alga, generic phytoplankton; Tele, *Teleaulax*; Meso, *Mesodinium*; Dino, *Dinophysis*; lDON, labile DON; slDON, semi-labile DON. The dashed line indicates the total nitrogen loading under oligotrophic conditions as a reference for the other simulations that have a different *y*-axis scale. The column labeled "*Dinophysis* grazer" shows the same simulations as the column "organisms" except now with the closure grazing function applied to *Dinophysis*. The complete test conditions are listed in **Table 4**.

of the organisms of prey and predator and competitors for nutrients alongside nutrient regeneration all impacted the dynamics. Consistent with Gaedke et al. (2010) who found biotic interactions in phytoplankton blooms to be highly complex with the potential to overrule climate change effects, our results indicate that the biotic interactions between the mixoplankton species in the TMD-complex to be a key factor in their response to environmental changes and thus need to be considered in predictions about the effect on climate change on this plankton.

The organisms in this model were configured as *Teleaulax amphioxeia*, *Mesodinium rubrum,* and *Dinophysis acuminata* as those were the TMD-complex species with the most physiological data available in published literature. However, the model can be configured to represent any species of the genus *Teleaulax*, *Mesodinium,* or *Dinophysis*, provided there are available data. The dynamic risk analysis showed the model to be sensitive to variations in the maximum growth rate (which is sensitive to temperature) as well as the pSNCM maximum plastid retention time (*crit_IR*) and the optimal prey capture rates (**Supplementary Data Sheet 1 Figure S1**). Different species of *Dinophysis* are known to vary in their physiology and ecology and toxin production (**Table 2** and **Supplementary Data Sheet 1 Table S1**; Reguera et al., 2012; García-Portela et al., 2018). Also, the plastid retention time may differ between species of *Dinophysis*. With more data becoming available on different species of the TMD-complex, the model could be used for exploring the potential implications of trait differences between the different species.

Apart from physiological and morphological variations, species of *Dinophysis* differ in seasonality, geographical distribution (**Figure 1**), and the hydrodynamics that support their proliferation (Reguera et al., 2012; Cusack et al., 2016; García-Portela et al., 2018). For example, in Australia, seasonal stratification and nutrient loads were found to be triggers for blooms of *D. acuminata*, while growths of *Dinophysis caudata* were linked to nutrients, salinity, and dissolved oxygen (Ajani et al., 2016). The importance of the TMD-complex is seen associated with a common trait of most species of *Dinophysis* in which they seem more dependent on the availability of their prey *Mesodinium* than on light availability (Reguera et al., 2012). Below, we discuss different facets of the interactions as driven by abiotic and biotic forcing as revealed in our simulations.

Predator-Prey Ratio Within the *Teleaulax-Mesodinium-Dinophysis*-Complex

Above all else, the ratio of encounters between the constituents of the TMD-complex affect the dynamics. Unlike CM (which may not need to feed regularly, if at all) or generalist non-constitutive mixoplankton (GNCM; which need to feed very frequently), pSNCM species, such as *Mesodinium* and *Dinophysis*,

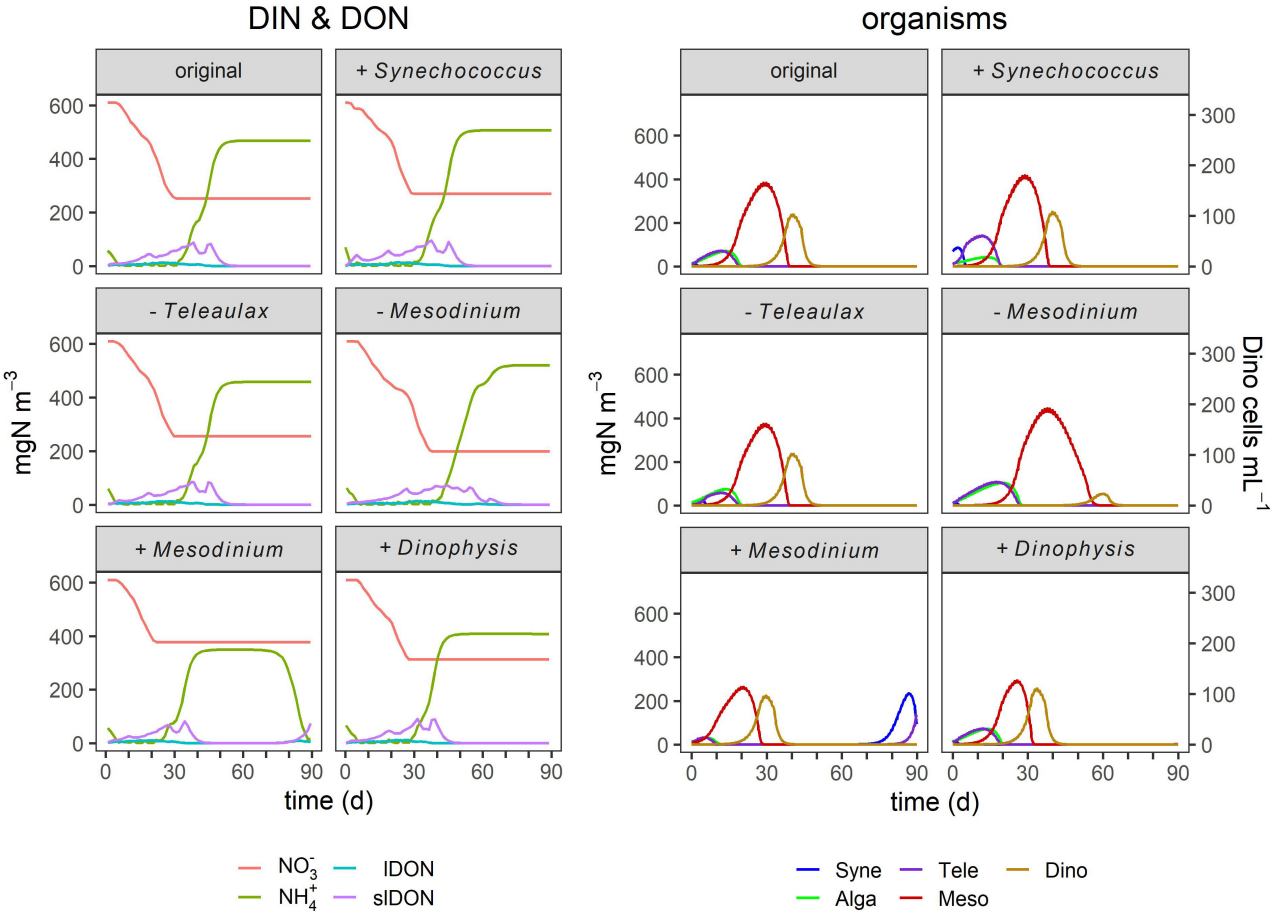

FIGURE 5 | Effect of initial organism ratios on TMD dynamics. These simulations were conducted as for **Figure 4**, with different nutrient loads, but now with higher ("+") or lower ("−") inocula. The panels labeled "original" are replicated from **Figure 4**, as default (control). The complete list of conditions and details of the simulations are listed in **Table 4** and described in the legend of **Figure 4**.

need to feed regularly but not necessarily frequently on their plastid donors. The initial ratio of the organisms at the start of simulations had a considerable impact on the subsequent bloom dynamics (**Figures 3**, **5**). The concentrations of *Mesodinium* in comparison to the other organisms appeared to have the biggest impact on overall bloom dynamics as the ciliate is both an important grazer on *Teleaulax* as well as being the specialist prey for acquired phototrophy to *Dinophysis*. However, the results were sometimes counter-intuitive as low initial concentrations of *Mesodinium* could result in comparatively low biomasses of *Dinophysis* while the ciliate itself subsequently grew to larger numbers (**Figure 3**). If the *Mesodinium* started out in low numbers in comparison to *Dinophysis*, the dinoflagellate was starved of sufficient plastids to support its population early on. At the same time, *Teleaulax* could develop larger cell numbers due to a lower grazing pressure by *Mesodinium*. By the time the cell numbers of *Mesodinium* increased, the ciliate found itself in perfect conditions with high biomass of its prey *Teleaulax* and low grazing pressure by *Dinophysis*. While *M. rubrum* is considered non-toxic, it is known to form large blooms (red-colored tides) that can, on collapse, lead to oxygen depletion and thus suffocation of other organisms (Yoo et al., 1998). *Dinophysis acuminata* is thus dependent both on the concentration of *M. rubrum* as well as the timing of its appearance. Prey availability early on in the growth phase of *Dinophysis* in the simulations appears to be crucial as the pSNCM will be able to maintain its chloroplasts for a time. In this situation, the relative and absolute amounts of the TMD-complex species are affected by nutrient loading, irradiance, and temperature.

Nutrient Loading

Our results suggest that eutrophic conditions increase the potential for *Dinophysis* blooms because these conditions prepare the system for larger *Mesodinium* blooms which then increase the potential for *Dinophysis* blooms (**Figures 3**, **4**). The importance of prey abundance for *Dinophysis* has been observed in the field (Moita et al., 2016; Smith et al., 2018), and DSP events have been related to high levels of dissolved organic and inorganic nutrients (Hattenrath-Lehmann et al., 2015; Hattenrath-Lehmann and Gobler, 2015). In the simulations, by the time *Dinophysis* starts to bloom, levels of nitrate could already be very low with

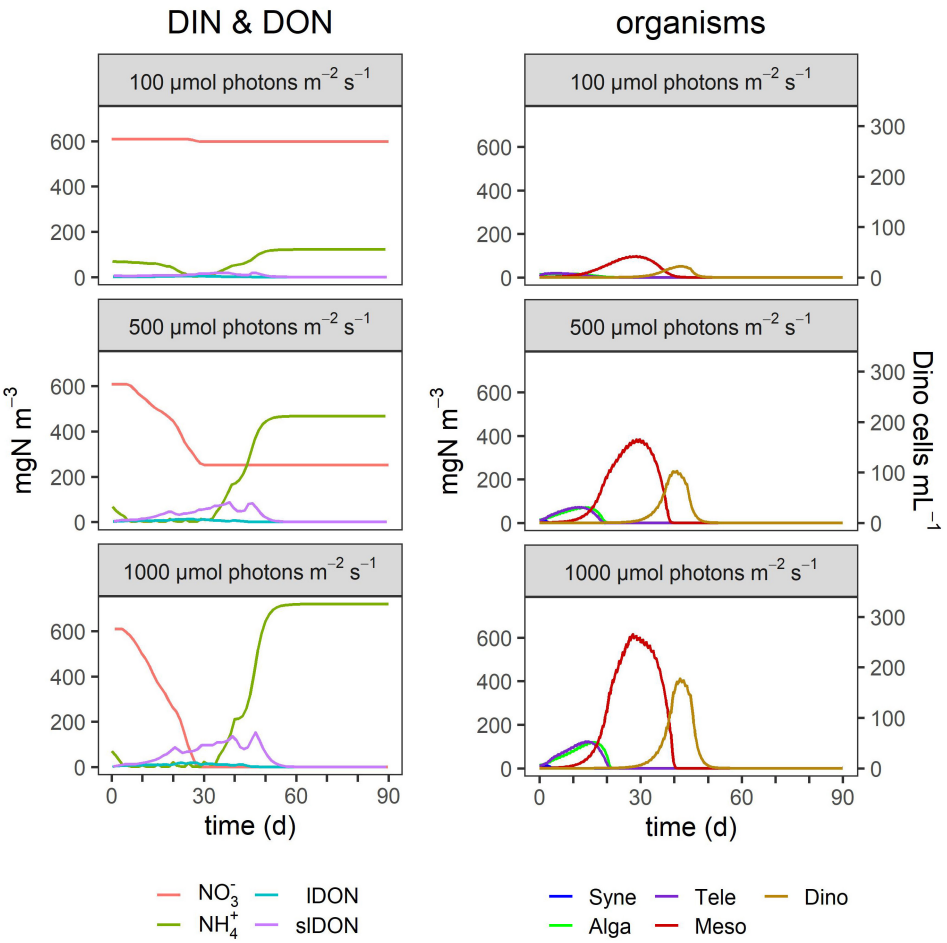

FIGURE 6 | Effect of surface irradiance on TMD dynamics. The outputs for 500 µmol photons m^{-2} s^{-1} replicate the conditions used for **Figure 4**. Other details as given in **Table 4** and in the legend of **Figure 4**.

ammonium starting to accumulate as a result of decomposition of lDON and slDON; this supported the growth of *Dinophysis* that had access to plenty of *Mesodinium* as a source for plastids. *Dinophysis* itself appears either unable or poorly equipped to use nitrate (Hattenrath-Lehmann et al., 2015; García-Portela et al., 2020); thus, in this study, we disabled the use of nitrate by *Dinophysis* (**Figure 2**). In any case, the intracellular regeneration of ammonium within *Dinophysis* on account of its feeding and then, later the increasing availability of external DON and ammonium would likely repress any significant need to use nitrate. *Dinophysis* has been found successfully growing in nitrogen-depleted waters (Seeyave et al., 2009). Thus, elevated nutrients have an indirect impact on *Dinophysis* blooms *via* the promotion of *Mesodinium* growth, plus a potential direct effect. This duality of direct and indirect effects of eutrophication on *Dinophysis* blooms also finds support by experimental studies on *D. acuminata* and *M. rubrum* (Hattenrath-Lehmann et al., 2015; Hattenrath-Lehmann and Gobler, 2015).

Anschütz and Flynn (2020) showed, through *in silico* experiments, that good growth conditions allow blooms of SNCM of such a magnitude that the essential provider of acquired phototrophy (e.g., *Teleaulax* for *Mesodinium*) is driven to extinction, and then, the SNCM bloom subsequently also becomes extinct (or the organism is forced to encyst). Lower nutrient systems prevent boom-and-bust dynamics and thus can support lower (but perhaps still actionable) levels of *Dinophysis*. The implication is that decreasing sources of eutrophication need not necessarily remove the potential for harmful blooms of *Dinophysis*.

With the exception of the simulations at different nutrient loads shown in **Figure 4**, the simulations were run without grazing on *Dinophysis* to focus on the effect of the interactions of *Teleaulax*, *Mesodinium,* and *Dinophysis* on their respective bloom dynamics. In the field, *Dinophysis* is subjected to grazing by protists (e.g., *Fragilidium*; Park and Kim, 2010) and metazoan zooplankton (e.g., copepods; Kozlowsky-Suzuki et al., 2006), which keeps their cell numbers lower. The activity of such grazers can be a major factor leading to the decline of *Dinophysis* blooms, together with changes in hydrodynamic characteristics of the water column (Escalera et al., 2010; Velo-Suárez et al., 2010). In our TMD-complex simulator, applying a generic encounter-based grazing rate to *Dinophysis* (**Figure 4**)

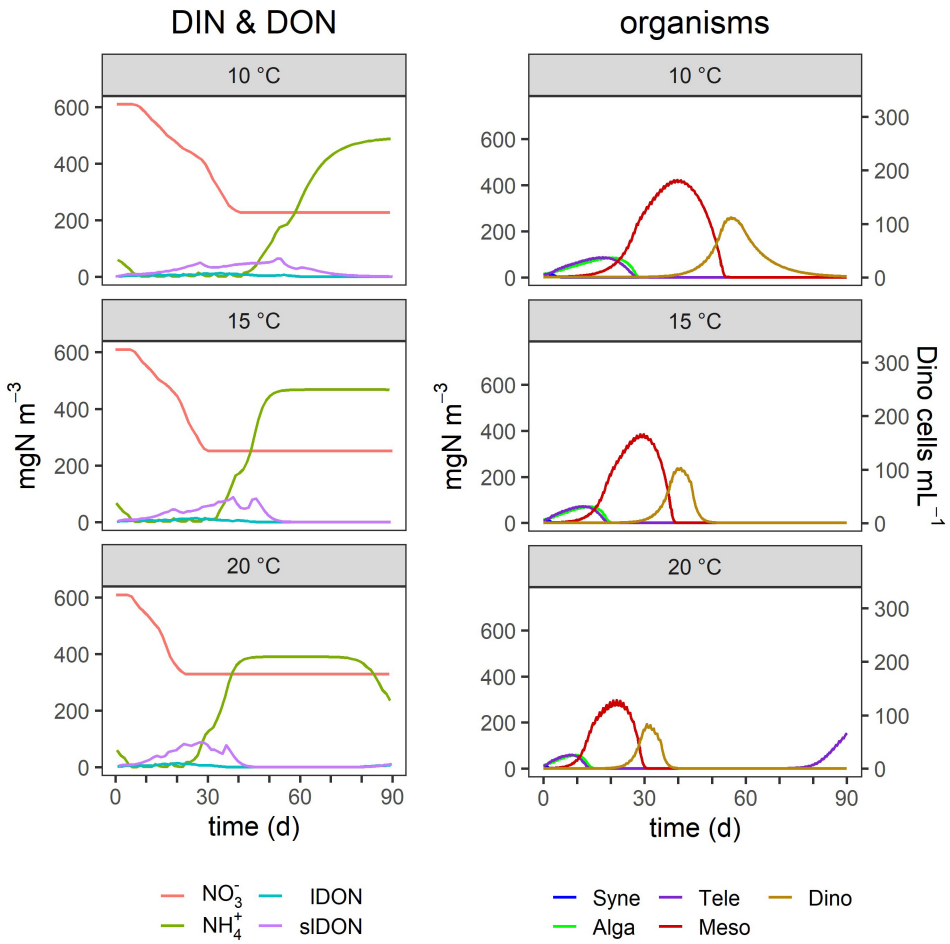

FIGURE 7 | Effect of temperature on TMD dynamics. The outputs for 15°C replicate the conditions used for **Figure 4**. Other details as given in **Table 4** and in the legend of **Figure 4**.

at different nutrient loads did not affect the maximum biomass of *Synechococcus*, *Teleaulax,* or *Mesodinium* and only prolonged the bloom phase of *Mesodinium* for a few days under eutrophic conditions. The timing and duration of blooms of *Dinophysis* did not change but the maximum cell numbers were lower. While grazing has clear potential to constrain *Dinophysis* numbers, ultimately, the absence of the *Mesodinium* required to furnish plastids for acquired phototrophy prevents *Dinophysis* growth. Our study suggests that the mixoplanktonic nutritional mode is a key to explain the seasonal lag of these blooms reported in the literature (Álvarez-Salgado et al., 2011).

Irradiance

Our simulations indicate that light is not a major factor affecting bloom duration, but it did affect the peak height (**Figure 3**) and thence, the overall dynamics. The model by Moeller et al. (2016), describing the interaction between the cryptophyte *Geminigera cryophila* (as the plastid donor) and *M. rubrum*, found that the need for acquired phototrophy affected the coexistence of the organism with its *G. cryophila* prey, such that increased irradiance shifted a stable coexistence to boom and bust cycles. Our simulations, portraying the entire TMD-complex, showed that such an interaction extended further to *Dinophysis*. However, while the maximum biomasses of *Teleaulax*, *Mesodinium,* and *Dinophysis* increased significantly with elevated irradiance (**Figure 3**), the boom and bust dynamic did not repeat in cycles (**Figure 6**). For *Teleaulax*, increased irradiance shortened the bloom duration (**Figure 3**) by accelerating their growth. Without a recurring reseeding (in nature, e.g., by advection), *Teleaulax* and *Mesodinium* were grazed to extinction, and *Dinophysis,* thus, could not take advantage of the increased nutrients. As noted above, the appearance of other predators grazing these organisms would also prevent a cycle from developing.

Higher irradiance has been found to decrease the time that *Dinophysis* can retain functional kleptochloroplasts in the absence of reacquisitions (Hansen et al., 2013). Irradiance may impact pSNCM growth by triggering photoacclimation in the acquired photosynthetic apparatus while decreasing their longevity due to photodamage. A higher level of photodamage may raise the demand for their specific prey to resupply plastids. Further developments of the TMD-complex simulator could include the implementation of an irradiance dependence of

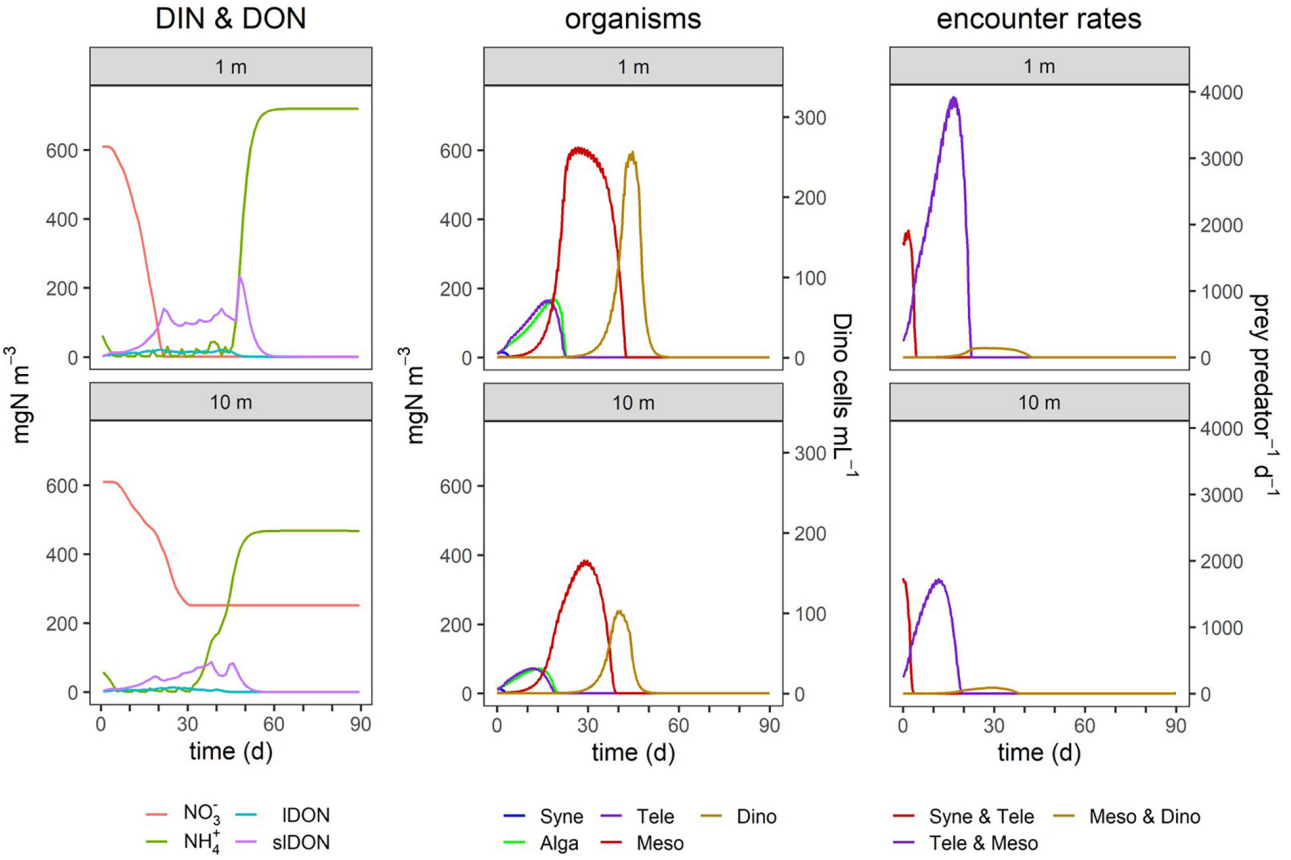

FIGURE 8 | TMD dynamics in simulated systems of different mixed layer depths (MLD). Simulations were run with an MLD of 10 m or 1 m, the latter simulating a thin layer; *Dinophysis* is often found in thin layers in stratified water columns where it is much easier to capture its fast prey *Mesodinium* due to much higher encounter rates. Encounter rates are of the three mixoplankton (*Teleaulax*, *Mesodinium*, and *Dinophysis*) with their respective prey, as shown in **Figure 2**. Other details as given in **Table 4** and in the legend of **Figure 4**.

the parameter *crit_IR* that controls the longevity of acquired phototrophy (**Supplementary Data Sheet 1 Table S3**), and photoacclimation could be simulated by changing the chlorophyll to carbon ratio (Chl:C). Photoacclimation is also known to be important to pSNCM growth in variable light (Moeller et al., 2016). Doing justice to this process and the decline of acquired phototrophy linked to both light and nutrient status requires models that better describe food quality that impacts on mixoplankton activity (e.g., Mitra and Flynn, 2010; Mitra et al., 2014; Lundgren et al., 2016; Lin et al., 2018). This requires the use of full variable stoichiometric (C:N:P:Chl) coarse-grain system biology-based ecosystem simulators (e.g., Flynn and Mitra, 2009; Leles et al., 2021).

Temperature

Temperature has a significant effect on the frequency of and extent of *Dinophysis* blooms (Escalera et al., 2006; Díaz et al., 2016; Pitcher et al., 2017). Temperature impacts are both abiotic and biotic. Warmer waters lead to a more stratified and stable water column that can favor *Dinophysis*. Such conditions are expected to become more frequent with climate change (Sallée et al., 2021). Temperature also increases metabolic rates, enacted in our TMD-complex food-web model by reference to a Q_{10} factor (see the "Materials and Methods" section). Temperature affected the time frame of the simulated blooms of *Teleaulax*, *Mesodinium,* and *Dinophysis* and the timing consequentially impacted the likelihood and size of *Dinophysis* blooms (**Figure 7**). However, the elevated temperature did not necessarily result in the largest blooms of *Dinophysis* as it accelerated the growth phase of *Mesodinium* such that *Dinophysis* had less exposure time to its specific prey (**Figures 3**, **7**). The optimal matching of *Dinophysis* appearance and growth with that of *Mesodinium* appeared to be a critical factor for *Dinophysis*. While hydrodynamic events of stratification, advection, and upwelling are crucial factors for *Dinophysis* bloom events (Escalera et al., 2010; Raine et al., 2010; Ajani et al., 2016; Díaz et al., 2016), the components of the TMD-complex need to be present in the appropriate magnitude at the right time for *Dinophysis* blooms to develop and produce high cell abundances (González-Gil et al., 2010; Sjöqvist and Lindholm, 2011). *Mesodinium* species and many toxic species of *Dinophysis* occur globally from polar to tropical regions (**Figure 1**; Gustafson et al., 2000; Reguera et al., 2012) and are, thus, exposed and adapted to different climates. There are

some differences in the distribution of species of *Dinophysis*. The species *D. acuminata* is ubiquitous; *D. norvegica* is more common in temperate to boreal regions while *D. caudata* bloom in tropical and subtropical regions (**Figure 1**; Reguera et al., 2012). It is unknown what effect climate change will have on the species distribution of *Dinophysis*. Furthermore, climate change will have different effects in these regions related to currents, upwelling and downwelling, stratification, and ocean acidification. Integrating the TMD-complex system dynamics model presented in this study, within a climate model could help to address these questions and lead to interesting new results in the research of these organisms.

Mixed Layer Depth and Advection

The MLD affects the way that light, nutrients, organism abundance, and temperature impact plankton ecology. The model simulated average biomass levels, while in reality, both *Mesodinium* and *Dinophysis* form aggregations that will affect encounter rates. *Dinophysis* often aggregate in very high abundances in thin layers (Campbell et al., 2010; González-Gil et al., 2010; Sjöqvist and Lindholm, 2011; Hattenrath-Lehmann et al., 2013; Díaz et al., 2016; Berdalet et al., 2017; Baldrich et al., 2021) that may even resemble monocultures (Farrell et al., 2012). This strategy increases encounter rates with their much faster prey enabling the *Dinophysis* to launch its ambush-style attacks on *Mesodinium* (Jiang et al., 2018). Turbulence damages ciliates (Smayda, 2002), and *M. rubrum* is documented to actively avoid turbulence (Cloern et al., 1994). In fact, the vertical stability of the water column is essential to enable *M. rubrum* to reach the highest cell abundances (Sanders, 1995; Herfort et al., 2011). Thus, stable water conditions may coincidentally favor the growth of their *Dinophysis* predator.

Simulations of conditions in a narrow band at depth (**Figure 8**) show how the formation of hydrodynamic conditions conducive to the formation of *Dinophysis* layers has the potential to mimic the consequences of bulk-water eutrophication in raising *in situ* predator-prey encounters. Mixoplanktonic activity provides a route to compensate for a lack of photosynthate in especially eutrophic conditions where the high biomass simultaneously shades light and provides high abundances of potential prey. Both the pSNCM species (*Mesodinium* and *Dinophysis*) encountered much more prey in the simulated 1-m thickness layer. For *Mesodinium* and especially *Dinophysis,* this led to a much higher biomass yield.

Diarrhetic shellfish poisoning events are often associated with the physical transport of *Dinophysis* populations by wind-driven advection and coastal counter-currents (Escalera et al., 2010; Raine et al., 2010; Reguera et al., 2012); therefore, the forecasting power of physical models for HAB events are linked to hydrodynamics (Raine et al., 2010; Velo-Suárez et al., 2010; Savvidis et al., 2011; Cusack et al., 2016; Moita et al., 2016; Pinto et al., 2016). In addition to horizontal currents, blooms have also been related to upwellings potentially bringing populations of *Dinophysis* from shelf bottom waters to the surface water and into (continued or enhanced) contact with their *M. rubrum* prey (Velo-Suárez et al., 2014). These flows also seed the surface water with different organisms in different proportions. These are conditions that influence factors, which our model suggests, can promote the development of *Dinophysis* blooms. Impacts of each member of the TMD-complex (and of course additional interactions on those members, such as predation and competition) all play parts in the story. The increase in stratification and MLD in the summertime due to climate change (Sallée et al., 2021) will likely also affect the bloom potential of *Dinophysis*. A changing ocean may challenge the reliability of existing forecasting models that are based on time-series data of hydrodynamic events. A solution could be mechanistic models that combine hydrodynamics and the biology of the TMD-complex components and allied species.

CONCLUSION

While our study shows the importance of prey availability for the growth of *Dinophysis*, it also shows that the timing of prey availability has a significant effect on the spatiotemporal dynamics of the TMD-complex. Simulations of the mixoplanktonic activity of these mixoplankton, configured in this study against data for *D. acuminata* and its prey *M. rubrum*, both with their special needs for acquired phototrophy, play an important role in the dynamics of bloom formation. Both high *M. rubrum* to *D. acuminata* ratios and the growth phase in which *D. acuminata* encounters *M. rubrum* are expected to affect cell abundances of *D. acuminata* in subsequent blooms. Even though they are not simulated in this study, it is very likely that these effects extend to other species from the genera *Mesodinium* and *Dinophysis* that share a similar relationship within cryptophyte-MD-complex. Monitoring programs for *Dinophysis* could, therefore, benefit from including *Mesodinium* in their routine observations; this has the advantage that *Mesodinium* appears in much larger numbers making it easier to detect than the cryptic *Dinophysis*. The disparity between monitoring and research efforts expended on just the terminal end of the TMD-complex (i.e., on *Dinophysis*) is notable. The other critical components, namely, *Mesodinium* and *Teleaulax*, receive far less attention (**Figure 1**) and yet their success and timing set the scene for blooms of the toxigenic species.

The dynamics shown by the simulations will perhaps act to prompt more attention in monitoring these other species. For aquaculture, it is not only important to know when the blooms will occur but also their duration. While the main reasons for the decline in *Dinophysis* blooms are often linked to dispersion (Velo-Suárez et al., 2010), grazing (Kozlowsky-Suzuki et al., 2006), and infections with parasites like *Amoebophrya* sp. (Velo-Suárez et al., 2014), a collapse in *Mesodinium* will inevitably lead to a failure in the *Dinophysis* a few weeks later just like an appearance of a *Mesodinium* bloom could indicate the potential for development of a harmful bloom of *Dinophysis*.

The *in silico* food-web simulator we used in this study may help to test sensitive parameters of different species and theoretically explore their behavior and inspire future experiments. The TMD-complex provides an interesting and

closely coupled example of successional interactions, and our model, thus, provides a tool to explore reasons for differences in bloom dynamics between species. As a nitrogen-based model, this simulator is also suitable for implementation in larger nitrogen-based ecosystem models and, therefore, exploration of TMD-complex dynamics and impacts in a larger context. The model presented in this study cannot replace a hydrodynamic model and on its own is not sufficient as a predicting tool for *Dinophysis* blooms occurring in the field. It is, however, the first biological model featuring *Teleaulax*, *Mesodinium,* and *Dinophysis*. This model could deliver useful results in combination with a hydrodynamic model that can account for stratification and *Dinophysis* input *via* currents from the outside (from offshore or up the coastline).

DATA AVAILABILITY STATEMENT

The original contributions presented in the study are included in the article/**Supplementary Material**, further inquiries can be directed to the corresponding author.

AUTHOR CONTRIBUTIONS

AM and KJF conceived the original idea. A-AA ran the simulations under the supervision of KJF and AM. All authors contributed to the construction of the models, analysis of the results, and writing of the manuscript.

FUNDING

This research was undertaken within the MixITiN project. This project has received funding from the European Union's Horizon 2020 Research and Innovation Program under the Marie Skłodowska-Curie Grant Agreement No. 766327. AM was supported by MixITiN and Sêr Cymru II WEFO ERDF Programme MixoHUB 82372.

SUPPLEMENTARY MATERIAL

The Supplementary Material for this article can be found online at: https://www.frontiersin.org/articles/10.3389/fmars.2021.799358/full#supplementary-material

REFERENCES

Ajani, P., Larsson, M. E., Rubio, A., Bush, S., Brett, S., and Farrell, H. (2016). Modelling bloom formation of the toxic dinoflagellates *Dinophysis acuminata* and *Dinophysis caudata* in a highly modified estuary, south eastern Australia. *Estuar. Coast. Shelf Sci.* 183, 95–106. doi: 10.1016/J.ECSS.2016.10.020

Alldredge, A. L., Passow, U., and Logan, B. E. (1993). The abundance and significance of a class of large, transparent organic particles in the ocean. *Deep Sea Res. Part I Oceanogr. Res. Pap.* 40, 1131–1140. doi: 10.1016/0967-0637(93)90129

Álvarez-Salgado, X. A., Figueiras, F. G., Fernández-Reiriz, M. J., Labarta, U., Peteiro, L., and Piedracoba, S. (2011). Control of lipophilic shellfish poisoning outbreaks by seasonal upwelling and continental runoff. *Harmful Algae* 10, 121–129. doi: 10.1016/j.hal.2010.08.003

Anderson, D. M., Glibert, P. M., and Burkholder, J. M. (2002). Harmful algal blooms and eutrophication: nutrient sources, compositions, and consequences. *Estuaries* 25, 704–726. doi: 10.1016/j.hal.2008.08.017

Anderson, D. M., Pitcher, G. C., and Estrada, M. (2005). The comparative "Systems" approach to HAB research. *Oceanography* 18, 148–157.

Anschütz, A. A., and Flynn, K. J. (2020). Niche separation between different functional types of mixoplankton: results from NPZ - style N - based model simulations. *Mar. Biol.* 167, 1–21. doi: 10.1007/s00227-019-3612-3

Baldrich, ÁM., Pérez-Santos, I., Álvarez, G., Reguera, B., Fernández-Pena, C., Rodríguez-Villegas, C., et al. (2021). Niche differentiation of *Dinophysis acuta* and *D. acuminata* in a stratified fjord. *Harmful Algae* 103:102010. doi: 10.1016/j.hal.2021.102010

Bérard-Therriault, L., Poulin, M., and Bossé, L. (1999). *Guide d'identification du phytoplancton marin de l'estuaire et du golfe du Saint-Laurent: incluant également certains protozoaires*. Ottawa: Les Presses Scientifiques du CNRC.

Berdalet, E., Reguera, B., Roy, S., Yamazaki, H., Cembella, A., and Raine, R. (2017). Harmful algal blooms in fjords, coastal embayments, and stratified systems: recent progress and future research. *Oceanography* 30, 46–57. doi: 10.5670/oceanog.2017.109

Blauw, A. N., Anderson, P., Estrada, M., Johansen, M., Laanemets, J., Peperzak, L., et al. (2006). The use of fuzzy logic for data analysis and modelling of European harmful algal blooms: results of the HABES project. *Afr. J. Mar. Sci.* 28, 365–369.

Broddrick, J. T., Welkie, D. G., Jallet, D., Golden, S. S., Peers, G., and Palsson, B. O. (2019). Predicting the metabolic capabilities of *Synechococcus* elongatus PCC 7942 adapted to different light regimes. *Metab. Eng.* 52, 42–56. doi: 10.1016/j.ymben.2018.11.001

Bronk, D. (1999). Rates of NH_4^+ uptake, intracellular transformation and dissolved organic nitrogen release in two clones of marine *Synechococcus* spp. *J. Plankton Res.* 21, 1337–1353. doi: 10.1093/plankt/21.7.1337

Campbell, L., and Carpenter, E. J. (1986). Diel patterns of cell division in marine *Synechococcus* spp. (*Cyanobacteria*): use of the frequency of dividing cells technique to measure growth rate. *Mar. Ecol. Prog. Ser.* 32, 139–148.

Campbell, L., Olson, R. J., Sosik, H. M., Abraham, A., Henrichs, D. W., Hyatt, C. J., et al. (2010). First harmful *Dinophysis* (*Dinophyceae*, *Dinophysiales*) bloom in the U.S. is revealed by automated imaging flow cytometry. *J. Phycol.* 46, 66–75. doi: 10.1111/j.1529-8817.2009.00791.x

Cloern, J. E., Cole, B. E., and Hager, S. W. (1994). Notes on a *Mesodinium rubrum* red tide in San Francisco Bay (California, USA). *J. Plankton Res.* 16, 1269–1276. doi: 10.1093/plankt/16.9.1269

Cusack, C., Dabrowski, T., Lyons, K., Berry, A., Westbrook, G., Salas, R., et al. (2016). Harmful algal bloom forecast system for SW Ireland. Part II: are operational oceanographic models useful in a HAB warning system. *Harmful Algae* 53, 86–101. doi: 10.1016/j.hal.2015.11.013

Díaz, P. A., Fernández-Pena, C., Pérez-Santos, I., Baldrich, Á, Díaz, M., and Rodríguez, F. (2020). *Dinophysis* Ehrenberg (*Dinophyceae*) in Southern Chile harbours red cryptophyte plastids from *Rhodomonas*/*Storeatula* clade. *Harmful Algae* 99:101907. doi: 10.1016/j.hal.2020.101907

Díaz, P. A., Ruiz-Villarreal, M., Pazos, Y., Moita, T., and Reguera, B. (2016). Climate variability and *Dinophysis acuta* blooms in an upwelling system. *Harmful Algae* 53, 145–159. doi: 10.1016/j.hal.2015.11.007

Escalera, L., Reguera, B., Moita, T., Pazos, Y., Cerejo, M., Cabanas, J. M., et al. (2010). Bloom dynamics of *Dinophysis acuta* in an upwelling system: in situ growth versus transport. *Harmful Algae* 9, 312–322. doi: 10.1016/j.hal.2009.12.002

Escalera, L., Reguera, B., Pazos, Y., Moroño, A., and Cabanas, J. M. (2006). Are different species of *Dinophysis* selected by climatological conditions? *Afr. J. Mar. Sci.* 28, 283–288. doi: 10.2989/18142320609504163

Farrell, H., Gentien, P., Fernand, L., Lunven, M., Reguera, B., González-Gil, S., et al. (2012). Scales characterising a high density thin layer of *Dinophysis acuta* Ehrenberg and its transport within a coastal jet. *Harmful Algae* 15, 36–46. doi: 10.1016/j.hal.2011.11.003

Fasham, M. J. R., Ducklow, H. W., and McKelvie, S. M. (1990). A nitrogen-based model of plankton dynamics in the oceanic mixed layer. *J. Mar. Res.* 48, 591–639. doi: 10.1357/002224090784984678

Flynn, K. J., and Butler, I. (1986). Nitrogen sources for the growth of marine microalgae: role of dissolved free amino acids. *Mar. Ecol. Prog. Ser.* 34, 281–304. doi: 10.3354/meps034281

Flynn, K. J., and McGillicuddy, D. J. (2018). "Modeling marine harmful algal blooms: current status and future prospects," in *Harmful Algal Blooms*, eds S. E. Shumway, J. M. Burkholder, and S. L. Morton (Chichester, UK: John Wiley & Sons, Ltd), 115–134. doi: 10.1002/9781118994672.ch3

Flynn, K. J., and Mitra, A. (2009). Building the "perfect beast": modelling mixotrophic plankton. *J. Plankton Res.* 31, 965–992. doi: 10.1093/plankt/fbp044

Flynn, K. J., and Mitra, A. (2016). Why plankton modelers should reconsider using rectangular hyperbolic (Michaelis-Menten, Monod) descriptions of predator-prey interactions. *Front. Mar. Sci.* 3:165. doi: 10.3389/fmars.2016.00165

Flynn, K. J., Mitra, A., Anestis, K., Anschütz, A. A., Calbet, A., Ferreira, G. D., et al. (2019). Mixotrophic protists and a new paradigm for marine ecology: where does plankton research go now? *J. Plankton Res.* 41, 375–391. doi: 10.1093/plankt/fbz026

Flynn, K. J., Stoecker, D. K., Mitra, A., Raven, J. A., Glibert, P. M., Hansen, P. J., et al. (2013). Misuse of the phytoplankton-zooplankton dichotomy: the need to assign organisms as mixotrophs within plankton functional types. *J. Plankton Res.* 35, 3–11. doi: 10.1093/plankt/fbs062

Franck, V., Bruland, K., Hutchins, D., and Brzezinski, M. (2003). Iron and zinc effects on silicic acid and nitrate uptake kinetics in three high-nutrient, low-chlorophyll (HNLC) regions. *Mar. Ecol. Prog. Ser.* 252, 15–33. doi: 10.3354/meps252015

Gaedke, U., Ruhenstroth-Bauer, M., Wiegand, I., Tirok, K., Aberle, N., Breithaupt, P., et al. (2010). Biotic interactions may overrule direct climate effects on spring phytoplankton dynamics. *Glob. Chang. Biol.* 16, 1122–1136. doi: 10.1111/j.1365-2486.2009.02009.x

García-Portela, M., Reguera, B., Gago, J., Le Gac, M., and Rodríguez, F. (2020). Uptake of inorganic and organic nitrogen sources by *Dinophysis acuminata* and *D. acuta*. *Microorganisms* 8:187. doi: 10.3390/microorganisms8020187

García-Portela, M., Riobó, P., Reguera, B., Garrido, J. L., Blanco, J., and Rodríguez, F. (2018). Comparative ecophysiology of *Dinophysis acuminata* and *D. acuta* (*Dinophyceae*, *Dinophysiales*): effect of light intensity and quality on growth, cellular toxin content, and photosynthesis. *J. Phycol.* 917, 899–917. doi: 10.1111/jpy.12794

Gentien, P., Lunven, M., Lehaître, M., and Duvent, J. L. (1995). *In-situ* depth profiling of particle sizes. *Deep Sea Res. Part I Oceanogr. Res. Pap.* 42, 1297–1312. doi: 10.1016/0967-0637(95)00058-E

Glibert, P. M., Allen, J. I., Bouwman, A. F., Brown, C. W., Flynn, K. J., Lewitus, A. J., et al. (2010). Modeling of HABs and eutrophication: status, advances, challenges. *J. Mar. Syst.* 83, 262–275. doi: 10.1016/j.jmarsys.2010.05.004

González-Gil, S., Velo-Suárez, L., Gentien, P., Ramilo, I., and Reguera, B. (2010). Phytoplankton assemblages and characterization of a *Dinophysis acuminata* population during an upwelling-downwelling cycle. *Aquat. Microb. Ecol.* 58, 273–286. doi: 10.3354/ame01372

Grobbelaar, N., Li, W.-T., and Huang, T.-C. (1991). Relationship between the nitrogenase activity and dark respiration rate of *Synechococcus* RF-1. *FEMS Microbiol. Lett.* 83, 99–102. doi: 10.1111/j.1574-6968.1991.tb04396.x

Gustafson, D. E., Stoecker, D. K., Johnson, M. D., Van Heukelem, W. F., and Sneider, K. (2000). Cryptophyte algae are robbed of their organelles by the marine ciliate *Mesodinium rubrum*. *Nature* 405, 1049–1052. doi: 10.1177/0956247816647344

Hamilton, M., Hennon, G. M. M., Morales, R., Needoba, J., Peterson, T. D., Schatz, M., et al. (2017). Dynamics of *Teleaulax*-like cryptophytes during the decline of a red water bloom in the Columbia River Estuary. *J. Plankton Res.* 39, 589–599. doi: 10.1093/plankt/fbx029

Hansen, P. J., Nielsen, L. T., Johnson, M., Berge, T., and Flynn, K. J. (2013). Acquired phototrophy in *Mesodinium* and *Dinophysis* - A review of cellular organization, prey selectivity, nutrient uptake and bioenergetics. *Harmful Algae* 28, 126–139. doi: 10.1016/j.hal.2013.06.004

Harred, L. B., and Campbell, L. (2014). Predicting harmful algal blooms: a case study with *Dinophysis ovum* in the Gulf of Mexico. *J. Plankton Res.* 36, 1434–1445. doi: 10.1093/plankt/fbu070

Hattenrath-Lehmann, T., and Gobler, C. J. (2015). The contribution of inorganic and organic nutrients to the growth of a North American isolate of the mixotrophic dinoflagellate, *Dinophysis acuminata*. *Limnol. Oceanogr.* 60, 1588–1603. doi: 10.1002/lno.10119

Hattenrath-Lehmann, T. K., Marcoval, M. A., Berry, D. L., Fire, S., Wang, Z., Morton, S. L., et al. (2013). The emergence of *Dinophysis acuminata* blooms and DSP toxins in shellfish in New York waters. *Harmful Algae* 26, 33–44. doi: 10.1016/j.hal.2013.03.005

Hattenrath-Lehmann, T. K., Marcoval, M. A., Mittlesdorf, H., Goleski, J. A., Wang, Z., Haynes, B., et al. (2015). Nitrogenous nutrients promote the prowth and toxicity of *Dinophysis acuminata* during estuarine bloom events. *PLoS One* 10:e0124148. doi: 10.1371/journal.pone.0124148

Herfort, L., Peterson, T. D., Campbell, V., Futrell, S., and Zuber, P. (2011). *Myrionecta rubra* (*Mesodinium rubrum*) bloom initiation in the Columbia River estuary. *Estuar. Coast. Shelf Sci.* 95, 440–446. doi: 10.1016/j.ecss.2011.10.015

Hernández-Urcera, J., Rial, P., García-Portela, M., Lourés, P., Kilcoyne, J., Rodríguez, F., et al. (2018). Notes on the cultivation of two mixotrophic *Dinophysis* species and their ciliate prey *Mesodinium rubrum*. *Toxins* 10, 505–505. doi: 10.3390/toxins10120505

Jaén, D., and Mamán, L. (2009). First report of *Dinophysis acuta* in culture. *Harmful Algae News* 39, 1–2.

Jeong, H. J., Lim, A. S., Franks, P. J. S., Lee, K. H., Kim, J. H., Kang, N. S., et al. (2015). A hierarchy of conceptual models of red-tide generation: nutrition, behavior, and biological interactions. *Harmful Algae* 47, 97–115. doi: 10.1016/j.hal.2015.06.004

Jiang, H., and Johnson, M. D. (2021). Swimming behavior of cryptophyte prey affects prey preference of the ambush-feeding ciliate *Mesodinium rubrum*. *Aquat. Microb. Ecol.* 86, 169–184. doi: 10.3354/ame01964

Jiang, H., Kulis, D. M., Brosnahan, M. L., and Anderson, D. M. (2018). Behavioral and mechanistic characteristics of the predator-prey interaction between the dinoflagellate *Dinophysis acuminata* and the ciliate *Mesodinium rubrum*. *Harmful Algae* 77, 43–54. doi: 10.1016/j.hal.2018.06.007

Johnson, M. D., and Stoecker, D. K. (2005). Role of feeding in growth and photophysiology of *Myrionecta rubra*. *Aquat. Microb. Ecol.* 39, 303–312.

Johnson, M. D., Tengs, T., Oldach, D., and Stoecker, D. K. (2006). Sequestration, performance, and functional control of cryptophyte plastids in the ciliate *Myrionecta rubra* (*ciliophora*). *J. Phycol.* 42, 1235–1246. doi: 10.1111/j.1529-8817.2006.00275.x

Kim, S., Kang, Y. G., Kim, H. S., Yih, W., Coats, D. W., and Park, M. G. (2008). Growth and grazing responses of the mixotrophic dinoflagellate *Dinophysis acuminata* as functions of light intensity and prey concentration. *Aquat. Microb. Ecol.* 51, 301–310. doi: 10.3354/ame01203

Kozlowsky-Suzuki, B., Carlsson, P., Rühl, A., and Granéli, E. (2006). Food selectivity and grazing impact on toxic *Dinophysis spp.* by copepods feeding on natural plankton assemblages. *Harmful Algae* 5, 57–68. doi: 10.1016/j.hal.2005.05.002

Larsen, J., and Moestrup, Ø (1992). "Potentially toxic phytoplankton. 2. Genus *Dinophysis* (*Dinophyceae*)," in *ICES Identification Leaflets for Plankton 180. International Council for the Exploration of the Sea*, ed. J. A. Lindley (Denmark, Copenhagen: ICES), 1–12.

Lee, B., and Park, M. G. (2017). Different life cycle strategies of the dinoflagellates *Fragilidium duplocampanaeforme* and its prey *Dinophysis acuminata* may explain their different susceptibilities to the infection by the parasite *Parvilucifera infectans*. *Harmful Algae* 65, 1–8. doi: 10.1016/j.hal.2017.04.002

Leles, S. G., Bruggeman, J., Polimene, L., Blackford, J., Flynn, K. J., and Mitra, A. (2021). Differences in physiology explain succession of mixoplankton functional types and affect carbon fluxes in temperate seas. *Prog. Oceanogr.* 190:102481. doi: 10.1016/j.pocean.2020.102481

Leles, S. G., Mitra, A., Flynn, K. J., Stoecker, D. K., Hansen, P. J., Calbet, A., et al. (2017). Oceanic protists with different forms of acquired phototrophy display contrasting biogeographies and abundance. *Proc. R. Soc. B* 284:20170664.

Lin, C.-H., Flynn, K. J., Mitra, A., and Glibert, P. M. (2018). Simulating effects of variable stoichiometry and temperature on mixotrophy in the harmful dinoflagellate *Karlodinium veneficum*. *Front. Mar. Sci.* 5:320. doi: 10.3389/fmars.2018.00320

Lundgren, V. M., Glibert, P. M., Granéli, E., Vidyarathna, N. K., Fiori, E., Ou, L., et al. (2016). Metabolic and physiological changes in *Prymnesium parvum*

when grown under, and grazing on prey of, variable nitrogen:phosphorus stoichiometry. *Harmful Algae* 55, 1–12. doi: 10.1016/j.hal.2016.01.002

Menden-Deuer, S., and Lessard, E. J. (2000). Carbon to volume relationships for dinoflagellates, diatoms, and other protist plankton. *Limnol. Oceanogr.* 45, 569–579.

Meunier, C. L., Schulz, K., Boersma, M., and Malzahn, A. M. (2013). Impact of swimming behaviour and nutrient limitation on predator-prey interactions in pelagic microbial food webs. *J. Exp. Mar. Biol. Ecol.* 446, 29–35. doi: 10.1016/j.jembe.2013.04.015

Mitra, A. (2009). Are closure terms appropriate or necessary descriptors of zooplankton loss in nutrient–phytoplankton–zooplankton type models? *Ecol. Modell.* 220, 611–620. doi: 10.1016/j.ecolmodel.2008.12.008

Mitra, A., and Flynn, K. J. (2010). Modelling mixotrophy in Harmful Algal Blooms; more or less the sum of the parts? *J. Mar. Syst.* 83, 158–169. doi: 10.1016/j.jmarsys.2010.04.006

Mitra, A., Flynn, K. J., Burkholder, J. M., Berge, T., Calbet, A., Raven, J. A., et al. (2014). The role of mixotrophic protists in the biological carbon pump. *Biogeosciences* 11, 995–1005. doi: 10.5194/bg-11-995-2014

Mitra, A., Flynn, K. J., Tillmann, U., Raven, J. A., Caron, D., Stoecker, D. K., et al. (2016). Defining planktonic protist functional groups on mechanisms for energy and nutrient acquisition: incorporation of diverse mixotrophic strategies. *Protist* 167, 106–120. doi: 10.1016/j.protis.2016.01.003

Moeller, H. V., Hsu, V., Lepori-Bui, M., Mesrop, L. Y., Chinn, C., and Johnson, M. D. (2021). Prey type constrains growth and photosynthetic capacity of the kleptoplastidic ciliate *Mesodinium chamaeleon* (*Ciliophora*). *J. Phycol.* 57, 916–930. doi: 10.1111/jpy.13131

Moeller, H. V., Johnson, M. D., and Falkowski, P. G. (2011). Photoacclimation in the phototrophic marine ciliate *Mesodinium rubrum* (*ciliophora*). *J. Phycol.* 47, 324–332. doi: 10.1111/j.1529-8817.2010.00954.x

Moeller, H. V., Peltomaa, E., Johnson, M. D., and Neubert, M. G. (2016). Acquired phototrophy stabilises coexistence and shapes intrinsic dynamics of an intraguild predator and its prey. *Ecol. Lett.* 19, 393–402. doi: 10.1111/ele.12572

Moita, M. T., Pazos, Y., Rocha, C., Nolasco, R., and Oliveira, P. B. (2016). Toward predicting *Dinophysis* blooms off NW Iberia: a decade of events. *Harmful Algae* 53, 17–32. doi: 10.1016/J.HAL.2015.12.002

Montagnes, D. J. S., Allen, J., Brown, L., Bulit, C., Davidson, R., Díaz-Ávalos, C., et al. (2008). Factors controlling the abundance and size distribution of the phototrophic ciliate *Myrionecta rubra* in open waters of the North Atlantic. *J. Eukaryot. Microbiol.* 55, 457–465. doi: 10.1111/j.1550-7408.2008.00344.x

Myung, G., Yih, W., Kim, H., Park, J., and Cho, B. (2006). Ingestion of bacterial cells by the marine photosynthetic ciliate *Myrionecta rubra*. *Aquat. Microb. Ecol.* 44, 175–180. doi: 10.3354/ame044175

Nam, S. W., Shin, W., Kang, M., Yih, W., and Park, M. G. (2015). Ultrastructure and molecular phylogeny of *Mesodinium coatsi* sp. nov., a benthic marine ciliate. *J. Eukaryot. Microbiol.* 62, 102–120. doi: 10.1111/jeu.12150

Nishitani, G., Nagai, S., Baba, K., Kiyokawa, S., Kosaka, Y., Miyamura, K., et al. (2010). High-level congruence of *Myrionecta rubra* prey and *Dinophysis* species plastid identities as revealed by genetic analyses of isolates from Japanese coastal waters. *Appl. Environ. Microbiol.* 76, 2791–2798. doi: 10.1128/AEM.02566-09

Olenina, I., Hajdu, S., Edler, L., Andersson, A., Wasmund, N., Busch, S., et al. (2006). Biovolumes and size-classes of phytoplankton in the Baltic Sea. *HELCOM Balt. Sea Environ. Proc.* 106, 1–144.

Park, J. H., Kim, M., Jeong, H. J., and Park, M. G. (2019). Revisiting the taxonomy of the "*Dinophysis acuminata* complex" (*Dinophyta*). *Harmful Algae* 88, 101657–101657. doi: 10.1016/j.hal.2019.101657

Park, M. G., and Kim, M. (2010). Prey specificity and feeding of the thecate mixotrophic dinoflagellate *Fragilidium duplocampanaeforme*. *J. Phycol.* 46, 424–432. doi: 10.1111/j.1529-8817.2010.00824.x

Park, M. G., Kim, S., Kim, H. S., Myung, G., Kang, Y. G., and Yih, W. (2006). First successful culture of the marine dinoflagellate *Dinophysis acuminata*. *Aquat. Microb. Ecol.* 45, 101–106. doi: 10.3354/ame045101

Park, M. G., Park, J. S., Kim, M., and Yih, W. (2008). Plastid dynamics during survival of *Dinophysis caudata* without its ciliate prey. *J. Phycol.* 44, 1154–1163. doi: 10.1111/j.1529-8817.2008.00579.x

Passow, U. (2002). Transparent exopolymer particles (TEP) in aquatic environments. *Prog. Oceanogr.* 55, 287–333. doi: 10.1016/S0079-6611(02)00138-6

Pinto, L., Mateus, M., and Silva, A. (2016). Modeling the transport pathways of harmful algal blooms in the Iberian coast. *Harmful Algae* 53, 8–16. doi: 10.1016/j.hal.2015.12.001

Pitcher, G. C., Jiménez, A. B., and Reguera, B. (2017). Harmful algal blooms in eastern boundary upwelling systems: a GEOHAB Core Research Project. *Oceanography* 30, 22–35. doi: 10.5670/oceanog.2017.107

Prézelin, B. B., and Schofield, O. (1989). Blue-green light effects on light-limited rates of photosynthesis: relationship to pigmentation and productivity estimates for *Synechococcus* populations from the Sargasso Sea. *Mar. Ecol. Prog. Ser.* 54, 121–139.

Raine, R., McDermott, G., Silke, J., Lyons, K., Nolan, G., and Cusack, C. (2010). A simple short range model for the prediction of harmful algal events in the bays of southwestern Ireland. *J. Mar. Syst.* 83, 150–157. doi: 10.1016/j.jmarsys.2010.05.001

Rao, D. V. S., and Pan, Y. (1993). Photosynthetic characteristics of *Dinophysis norvegica* Claparede & Lachmann, a red-tide dinoflagellate. *J. Plankton Res.* 15, 965–976. doi: 10.1093/plankt/15.8.965

Reguera, B., Riobó, P., Rodríguez, F., Díaz, P. A., Pizarro, G., Paz, B., et al. (2014). *Dinophysis* toxins: causative organisms, distribution and fate in shellfish. *Mar. Drugs* 12, 394–461. doi: 10.3390/md12010394

Reguera, B., Velo-Suárez, L., Raine, R., and Park, M. G. (2012). Harmful *Dinophysis* species: a review. *Harmful Algae* 14, 87–106. doi: 10.1016/j.hal.2011.10.016

Rial, P., Garrido, J. L., Jaén, D., and Rodríguez, F. (2013). Pigment composition in three *Dinophysis* species (*Dinophyceae*) and the associated cultures of *Mesodinium rubrum* and *Teleaulax amphioxeia*. *J. Plankton Res.* 35, 433–437. doi: 10.1093/plankt/fbs099

Rial, P., Laza-Martínez, A., Reguera, B., Raho, N., and Rodríguez, F. (2015). Origin of cryptophyte plastids in *Dinophysis* from Galician waters: results from field and culture experiments. *Aquat. Microb. Ecol.* 76, 163–174. doi: 10.3354/ame01774

Riisgård, H. U., and Larsen, P. S. (2009). Ciliary-propelling mechanism, effect of temperature and viscosity on swimming speed, and adaptive significance of "jumping" in the ciliate *Mesodinium rubrum*. *Mar. Biol. Res.* 5, 585–595. doi: 10.1080/17451000902729704

Rodríguez, F., Escalera, L., Reguera, B., Rial, P., Riobó, P., and de Jesús da Silva, T. (2012). Morphological variability, toxinology and genetics of the dinoflagellate *Dinophysis tripos* (*Dinophysiaceae*, *Dinophysiales*). *Harmful Algae* 13, 26–33. doi: 10.1016/j.hal.2011.09.012

Ruiz-Villarreal, M., García-García, L. M., Cobas, M., Díaz, P. A., and Reguera, B. (2016). Modelling the hydrodynamic conditions associated with *Dinophysis* blooms in Galicia (NW Spain). *Harmful Algae* 53, 40–52. doi: 10.1016/j.hal.2015.12.003

Sallée, J.-B., Pellichero, V., Akhoudas, C., Pauthenet, E., Vignes, L., Schmidtko, S., et al. (2021). Summertime increases in upper-ocean stratification and mixed-layer depth. *Nature* 591, 592–598. doi: 10.1038/s41586-021-03303-x

Sanders, R. (1995). Seasonal distributions of the photosynthesizing ciliates *Laboea strobila* and *Myrionecta rubra* (= *Mesodinium rubrum*) in an estuary of the Gulf of Maine. *Aquat. Microb. Ecol.* 9, 237–242. doi: 10.3354/ame009237

Savvidis, Y. G., Patoucheas, D. P., Nikolaidis, G., and Koutitas, C. G. (2011). Modelling the dispersion of harmful algal bloom (HAB) in the Thermaikos Gulf (NW Aegean Sea). *Glob. Nest J.* 13, 119–129. doi: 10.30955/gnj.000670

Seeyave, S., Probyn, T. A., Pitcher, G. C., Lucas, M. I., and Purdie, D. A. (2009). Nitrogen nutrition in assemblages dominated by *Pseudo-nitzschia* spp., *Alexandrium catenella* and *Dinophysis acuminata* off the west coast of South Africa. *Mar. Ecol. Prog. Ser.* 379, 91–107. doi: 10.3354/meps07898

Singh, A., Hårding, K., Reddy, H. R. V., and Godhe, A. (2014). An assessment of *Dinophysis* blooms in the coastal Arabian Sea. *Harmful Algae* 34, 29–35.

Sjöqvist, C. O., and Lindholm, T. J. (2011). Natural co-occurrence of *Dinophysis acuminata* (*Dinoflagellata*) and *Mesodinium rubrum* (*Ciliophora*) in thin layers in a coastal inlet. *J. Eukaryot. Microbiol.* 58, 365–372. doi: 10.1111/j.1550-7408.2011.00559.x

Smayda, T. J. (2002). Turbulence, watermass stratification and harmful algal blooms: an alternative view and frontal zones as "pelagic seed banks.". *Harmful Algae* 1, 95–112. doi: 10.1016/S1568-9883(02)00010-0

Smith, E. L. (1936). Photosynthesis in relation to light and carbon dioxide. *Proc. Natl. Acad. Sci. U. S. A.* 22, 504–511. doi: 10.1073/pnas.22.8.504

Smith, J. L., Tong, M., Kulis, D., and Anderson, D. M. (2018). Effect of ciliate strain, size, and nutritional content on the growth and toxicity of mixotrophic *Dinophysis acuminata*. *Harmful Algae* 78, 95–105. doi: 10.1016/j.hal.2018.08.001

Suzuki, T., Miyazono, A., Baba, K., Sugawara, R., and Kamiyama, T. (2009). LC-MS/MS analysis of okadaic acid analogues and other lipophilic toxins in single-cell isolates of several *Dinophysis* species collected in Hokkaido, Japan. *Harmful Algae* 8, 233–238.

Turpin, D. H., and Miller, A. G. (1985). Predicting the kinetics of dissolved inorganic carbon limited growth from the short-term kinetics of photosynthesis in *Synechococcus leopliensis* (Cyanophyta). *J. Phycol.* 21, 409–418.

Velo-Suárez, L., González-Gil, S., Pazos, Y., and Reguera, B. (2014). The growth season of *Dinophysis acuminata* in an upwelling system embayment: a conceptual model based on in situ measurements. *Deep-Sea Res. Part II Top. Stud. Oceanogr.* 101, 141–151. doi: 10.1016/j.dsr2.2013.03.033

Velo-Suárez, L., and Gutiérrez-Estrada, J. C. (2007). Artificial neural network approaches to one-step weekly prediction of *Dinophysis acuminata* blooms in Huelva (Western Andalucía, Spain). *Harmful Algae* 6, 361–371. doi: 10.1016/j.hal.2006.11.002

Velo-Suárez, L., Reguera, B., González-Gil, S., Lunven, M., Lazure, P., Nézan, E., et al. (2010). Application of a 3D Lagrangian model to explain the decline of a *Dinophysis acuminata* bloom in the Bay of Biscay. *J. Mar. Syst.* 83, 242–252. doi: 10.1016/j.jmarsys.2010.05.011

Wawrik, B., Callaghan, A. V., and Bronk, D. A. (2009). Use of inorganic and organic nitrogen by *Synechococcus* spp. and diatoms on the West Florida Shelf as measured using stable isotope probing. *Appl. Environ. Microbiol.* 75, 6662–6670. doi: 10.1128/AEM.01002-09

Yasumoto, T., Murata, M., Oshima, Y., Sano, M., Matsumoto, G. K., and Clardy, J. (1985). Diarrhetic shellfish toxins. *Tetrahedron* 41, 1019–1025.

Yih, W., Hyung, S. K., Hae, J. J., Myung, G., and Young, G. K. (2004). Ingestion of cryptophyte cells by the marine photosynthetic ciliate *Mesodinium rubrum*. *Aquat. Microb. Ecol.* 36, 165–170. doi: 10.3354/ame036165

Yoo, J.-S., Lee, J.-H., and Fukuyo, Y. (1998). Red tide organism: ciliate *Mesodinium rubrum* (Lohmann) Hamburger et Buddenbrock. *Algae* 13, 143–149.

Yoo, Y. D., Seong, K. A., Jeong, H. J., Yih, W., Rho, J.-R., Nam, S. W., et al. (2017). Mixotrophy in the marine red-tide cryptophyte *Teleaulax amphioxeia* and ingestion and grazing impact of cryptophytes on natural populations of bacteria in Korean coastal waters. *Harmful Algae* 68, 105–117. doi: 10.1016/j.hal.2017.07.012

Conflict of Interest: The authors declare that the research was conducted in the absence of any commercial or financial relationships that could be construed as a potential conflict of interest.